

Complexity dynamics analysis of a dual-channel green supply chain with government intervention and cap-and-trade regulation

Yuhao Zhang(张玉豪), Lin Huang(黄林), and Man Yang(杨满)

Citation: Chin. Phys. B, 2025, 34 (**7**): 070501. DOI: 10.1088/1674-1056/adca9c
Journal homepage: http://cpb.iphy.ac.cn; http://iopscience.iop.org/cpb

What follows is a list of articles you may be interested in

Enhancing phase separation of double-chiral particles by regulating inter-chiral frustration

Yi-Chen Lu(陆羿辰), Wan-Rou Cai(蔡婉柔), Meng-Chu Wang(王梦楚), Ya-Li Liu(刘雅莉), Tong Zhu(朱童), Yi-Lin Zhou(周怡琳), Tian-Chen Yu(余天晨), Yun-Xuan Ji(纪蕴轩), Ming-Qian Ao(敖明茜), Chen-Lu Li(李晨璐), Cheng-Xu Yan(颜乘旭), and Zhi-Gang Zheng(郑志刚)
Chin. Phys. B, 2025, 34 (**8**): 080506. DOI: 10.1088/1674-1056/ade06f

An enhanced fingerprint template protection scheme based on four-dimensional superchaotic system and dynamic DNA coding

Baiqiang Hu(胡百强), Jiahui Liu(刘嘉辉), Zhe Liu(刘喆)
Chin. Phys. B, 2025, 34 (**7**): 070505. DOI: 10.1088/1674-1056/adca9f

Bifurcation and chaos characteristics of hysteresis vibration system of giant magnetostrictive actuator

Hong-Bo Yan(闫洪波), Hong Gao(高鸿), Gao-Wei Yang(杨高炜), Hong-Bo Hao(郝宏波), Yu Niu(牛禹), Pei Liu(刘霈)
Chin. Phys. B, 2020, 29 (**2**): 020504. DOI: 10.1088/1674-1056/ab65b4

Bifurcation and chaos in high-frequency peak current mode Buck converter

Chang-Yuan Chang(常昌远), Xin Zhao(赵欣), Fan Yang(杨帆), Cheng-En Wu(吴承恩)
Chin. Phys. B, 2016, 25 (**7**): 070504. DOI: 10.1088/1674-1056/25/7/070504

Hysteresis-induced bifurcation and chaos in a magneto-rheological suspension system under external excitation

Hailong Zhang(张海龙), Enrong Wang(王恩荣), Fuhong Min(闵富红), Ning Zhang(张宁)
Chin. Phys. B, 2016, 25 (**3**): 030503. DOI: 10.1088/1674-1056/25/3/030503

Complexity dynamics analysis of a dual-channel green supply chain with government intervention and cap-and-trade regulation

Yuhao Zhang(张玉豪)[1], Lin Huang(黄林)[2,3,†], and Man Yang(杨满)[4]

[1] *School of Business, Jiangsu University of Science and Technology, Suzhou* 215600, *China*
[2] *School of Economics and Management, Huzhou University, Huzhou* 313000, *China*
[3] *Institute of Sustainable Development, Huzhou University, Huzhou* 313000, *China*
[4] *Logistics Engineering College, Shanghai Maritime University, Shanghai* 201306, *China*

(Received 29 October 2024; revised manuscript received 31 March 2025; accepted manuscript online 9 April 2025)

This paper studies a dual-channel green supply chain consisting of one manufacturer and one retailer in presence of government green subsidy and cap-and-trade regulation policies. We first develop and analyze a single-period Stackelberg and a multi-period dynamic Stackelberg game models respectively with consistent pricing strategy. Subsequently, we extend these two game models by utilizing an inconsistent pricing strategy. The optimal solutions for the single-period Stackelberg game models in both scenarios are derived by means of the backward induction approach. Moreover, the existence and local asymptotic stability of the equilibrium points of the multi-period dynamic Stackelberg game models are examined, and the complex dynamics of chain members' long-term strategy evolution are investigated through chaos theory and numerical simulation. Additionally, the variable feedback control and time-delay feedback control method are utilized to eliminate system chaos respectively. The results indicate that (i) The excessive fast adjustment speeds by the manufacturer have a destabilizing effect on the stability of the Nash equilibrium point. (ii) The manufacturer's profits are improved with green subsidy degree increases, while its impact on the retailer's profits depends on certain parameter conditions, and the high carbon trading price is disadvantage to both chain members. (iii) The system's motion can transition from a steady state to a chaotic period through period-doubling or Neimark–Sacker bifurcations. (iv) The system's steady state is conducive to the manufacturer, while the retailer can benefit from the system's periodic cycles. Furthermore, both chain members' profits are declined when the system becomes chaotic. Lastly, the variable feedback and time-delay feedback control method can effectively eliminate system chaos.

Keywords: dual-channel, green subsidy, cap-and-trade, Stackelberg game, bifurcation and chaos

PACS: 05.45.–a, 05.45.Pq

DOI: 10.1088/1674-1056/adca9c **CSTR:** 32038.14.CPB.adca9c

1. Introduction

In recent years, environmental pollution and global warming issues have received much more attention from many countries and regions worldwide, and carbon dioxide is regarded as the main factor that causes the greenhouse effects.[1] To cope with these problems, many carbon control regulations and legislations have been promulgated to curb carbon emission and reduce energy consumption, such as carbon taxes, carbon cap, carbon offset, and cap-and-trade policies, for achieving sustainable development and low-carbon circular economic.[2] For instance, China, the most carbon emission country in the world, has committed to reducing carbon emissions per unit of GDP by 60%–65% by 2030 compared to 2005,[3] and has promised to realize carbon peaking by 2030 and achieve carbon neutrality by 2060.[4,5] Moreover, both the United Kingdom and the United States have issued relevant policies to achieve the net-zero target by 2050.

Cap-and-trade regulation is considered as an effective mechanism, which is widely applied by many governments.[6] It is a market-based mechanism to control total emissions of enterprises.[7,8] Under such a policy, the government allocates carbon caps freely to the firms at the beginning age, and the firms can sell and purchase carbon credits in the carbon trading market at latter age.[1] This system stimulates enterprises to make more efforts in green technology investment and employ eco-friendly manner to produce greener products.

In response to carbon control regulations, many leading corporations consider green production as an essential business strategy in the market, including Apple, Gree, H & M, Marks & Spencer, Home Depot, and Panasonic Group, and so on, are eager to appeal more consumers who exhibit low-carbon preference, thereby have made more efforts in emissions reduction.[9] For instance, as a previous survey pointed out that in China, more than 65 million consumers prefer eco-friendly products[10] Consequently, Haier has proposed a four-stage green strategy committed to advancing the low-carbon upgrade of China's household electrical appliances, which greatly contributed to energy conservation and emissions reduction.[11] Therefore, it is vital and necessary to establish mathematical models to explore the influence of cap-

†Corresponding author. E-mail: lin-huang@163.sufe.edu.cn

© 2025 Chinese Physical Society and IOP Publishing Ltd. All rights, including for text and data mining, AI training, and similar technologies, are reserved.

and-trade policy on short-and long-term decisions of green investment and pricing within the dual-channel green supply chain.

In reality, to accelerate the manufacturers to invest in green technology and cleaner production rapidly, the government is willing to provide subsidies to the manufacturer based on the carbon emissions reduction degree per unit product or the emission abatement investment cost of the manufacturer. For instance, the Clean Technology Investment Program initiated by the Australian government shoulders up to 50% of the costs associated with investing in emission-reducing technologies.[12] There is no doubt that government green subsidy policy has a significant influence on pricing, emission reduction decisions and performance of chain members. Therefore, it is essential to develop mathematical models to explore the impact of government green subsidy on the short-and long-term strategies of chain members in the dual-channel green supply chain where the consumer exhibits low-carbon preference behaviors.

In addition, the rapid development and wide applied of Internet technology has promoted many enterprises to build direct sales channels (online channels), which is conducive to attracting more consumers who prefer to buy goods through online channels, thereby enhancing the market share of the product.[13] Dual-channel structure has become more popular channel structure and employed as an important business mode by many firms. However, the encroachment of direct sale channel of manufacturer will canalize the product sales in the traditional retail channel, which cause more intense competition between two distribution channels.[14] In order to alleviate channel competition for the dual-channel supply chain, the consistent pricing strategy is applied by many enterprises, such as Apple, Dell, IBM, and so on.[15]

An increasing number of scholars have discussed the optimal pricing and emission reduction decisions of green supply chain under the assumption of complete rationality. However, due to the complexities of market competition, chain members can rarely grasp all market information, thereby making decisions based on partial information and become bounded rational agents. To enhance performance, the bounded rational player needs to adjust his strategies in each game period based on the previous decision information of himself and the competitors. Therefore, the game process between chain members is the repeated game model. However, the long-term price and emission reduction strategies of dual-channel supply chain in presence of cap-and-trade regulation and green subsidy policies under bounded rationality remain unclear.

Our study concentrates on addressing the following research questions:

(i) What are the optimal channel pricing and emission reduction decisions for the dual-channel supply chain considering consumer environmental awareness and different pricing strategies under cap-and-trade and government green subsidy policies?

(ii) Under the bounded rationality rule, how do key parameters, including the adjustment speeds of channel price and emission abatement rate, green subsidy degree, and carbon trading price affect the stability features of equilibrium solutions and the complex dynamics of multi-period Stackelberg game models within the dual-channel green supply chain?

(iii) How does the performance of chain members vary in terms of different parameter conditions with different dynamical behaviors of the system?

To this end, we study a dual-channel green supply chain that incorporates cap-and-trade regulation and green subsidy policies, in which the manufacturer produces low-carbon products by employing emission-reducing technologies, and distributes them via both direct and traditional retail sale channels. We first establish and analyze a single-period Stackelberg game model with different pricing strategies under complete rationality. Furthermore, the single-period Stackelberg game models are extended into a multi-period Stackelberg game models with a gradient adjustment mechanism under bounded rationality. Additionally, the stability and complexity characteristics of chain members' long-run strategies are investigated, as well as performance of chain members under various parameter conditions are investigated by chaos theory and numerical simulation.

2. Literature review

Our work is closely related to three growing research streams, including the dual-channel supply chains game models with government subsidy policy, the dual-channel supply chain game models with cap-and-trade regulation, and the complex dynamics of supply chain game models.

2.1. Dual-channel supply chains game models with government intervention

An increasing number of works have investigated the influences of governmental green subsidy on the optimal decisions of green supply chains.[16,17] Meng *et al.*[18] proposed a dual-channel green supply chain models considering consumer green preference and channel preference within a dual-channel structure under the government subsidies policy. The optimal solutions of chain members are explored with collaborative pricing policies. The findings illustrated that government subsidies are beneficial to promoting the sales efforts of green products for the manufacturer. Barman *et al.*[19] proposed a dual-channel green supply chain consisting of one supplier, one manufacturer and one independent retailer, in which the government provides a subsidy to the manufacturer for green investment. The optimal pricing, greening level and

performance of chain members under consistent and inconsistent pricing strategies are compared. Zaefarian *et al.*[20] studied a dynamic game model in a green supply chain with two substitutable products considering demand disruption and government intervention under bounded rationality.

Although the above cited literature has investigated the effects of green subsidy policy on optimal price and emission reduction decisions of different dual-channel structures, most of them without considering the equilibrium solutions of chain members associated with different pricing strategies, i.e., consistent pricing and inconsistent pricing strategies. In addition, all of the aforesaid works have ignored cap-and-trade regulation, which has greatly reshaped operational decisions of the supply chain.

2.2. Supply chain game models with cap-and-trade regulation

Many scholars have paid more attention on exploring optimal decision and performance of the green supply chain under cap-and-trade regulation.[21–23] Several scholars investigated the impacts of cap-and-trade regulation on operational decisions of single-channel supply chain. Zhang *et al.*[24] studied optimal production strategy and emission abatement decisions of three game models considering different power structures and cap-and-trade policy. The research pointed that the high degree of the consumer's low-carbon preference and vertical Nash structure are more beneficial to the social welfare. Some works have discussed optimal strategies of chain members in the context of dual-channel situation. Barman *et al.*[21] investigated optimal decisions of channel prices, carbon reduction and delivery lead-time of online products in a dual-channel green supply chain under cap-and-trade policy, and a centralized and two Stackelberg game models are developed and analyzed. Li *et al.*[25] examined how the manufacturer makes joint decisions on the green product, pricing and the online selling modes in a dual-channel structure. The results indicated that agency selling mode is more profitable for the e-tailer when agency fee is low and moderate, and the higher consumer green awareness incentivizes the manufacturer to prefer agency selling.

Only a few scholars have studied the joint effect of government green subsidy and cap-and-trade regulation within the supply chain. Li *et al.*[7] investigated the combined effects of different government subsidy modes and cap-and-trade mechanism in a two-echelon green supply chain considering green technology investment. Three Stackelberg game models are analyzed and some numerical experiments are conducted. Chai *et al.*[26] analyzed the joint effects of government subsidy and cap-and-trade policies on remanufacturing in a closed-loop supply chain. Three stylized models associated with different subsidy policies are studied, but the work does not involve dual-channel situation. However, the abovementioned works only investigate the joint effect of green subsidy and cap-and-trade policies on short-term equilibrium solution with complete rationality, and also without involving the dual-channel circumstances.

Different from the existing literature, our work concentrates on examining the joint effects of government green subsidy and cap-and-trade policies on the dynamic strategies and its long-term evolution process of chain members in the dual-channel supply chain with different pricing strategies. Numerical experiments are utilized to reveal more important results and managerial enlightenments.

2.3. Complex dynamics of supply chain game models

A branch of research stream concentrates on studying complex dynamics of multi-period game models in supply chains,[27,28] and some scholars centers on studying complexity characteristics of dual-channel game models.[29–31] Zhang and Wang[32] investigated dynamic pricing strategies of decentralized and centralized game models by considering the retailer's service value within a dual-channel supply chain. The influence of key parameters on the system's stability and complex dynamical behavior of chain members are explored. Ma and Wang[5] based on a low-carbon apparel supply chain, the static and dynamic decision-making models under centralized and decentralized frameworks are constructed and analyzed. The complex dynamics of channel members' long-term strategies are examined by combining with local and global bifurcation theory. However, the above employed literature without considering the green subsidy and cap-and-trade policies. Some scholars have studied complex dynamics of dual-channel game models under cap-and-trade regulation, but the related works have no involving dual-channel situations.[33–35] However, by observing the existing works, research on the short-and long-term decisions of dual-channel green supply chain considering green subsidy and cap-and-trade regulation policies is quite scarce, especially, the pricing and emission reduction decisions of chain members under different pricing strategies should be further explored with complete and bounded rationality expectation respectively.

2.4. Research gaps and contributions

By reviewing the existing literature related to our study, we observe that several essential research questions need to be further discussed, the identified research gaps can be summarized as follows:

(i) Several scholars have explored the influence of governmental green subsidy or cap-and-trade regulation on optimal pricing and emission reduction decisions within dual-channel supply chain. Nevertheless, few works have addressed the combined effects of green subsidy and cap-and-trade policies on the optimal equilibrium solution, including pricing and

emission reduction decisions within a dual-channel green supply chain. Specifically, the optimal solutions associated with consistent pricing and inconsistent pricing strategies considering the government subsidy and cap-and-trade policies has not been discussed yet.

(ii) Some scholars have studied the combined effects of green subsidies and cap-and-trade regulation on optimal solutions in supply chains with complete rationality. However, there is a scarcity of studies focusing on investigating the long-term strategies and its complex dynamics of channel members with bounded rationality, especially within the dual-channel green supply chain.

In light of existing research gaps, our study centers on analyzing the outcomes of the single-period Stackelberg game model and the complex dynamics of multi-period Stackelberg game models considering consistent pricing and inconsistent pricing strategies respectively. Moreover, the profit levels of channel members in terms of different system motions are explored.

The research proposes and contributions of our work are as follows:

(I) Our study enriches the research body on dual-channel green supply chain operations management by incorporating governmental green subsidy and cap-and-trade policies under completely rationality expectation. The combined effects of these policies on the chain members' optimal equilibrium solutions are revealed. The research findings are conducive to improving the short-term competitive ability and performance of chain members.

(II) Our work is the first study to establish and analyze dynamic multi-period Stackelberg game models associated with different pricing strategies, and complex features of them and the long-term performance of channel members are explored with government green subsidy and cap-and trade policies. The derived conclusions and managerial implications can guide policymakers and chain members to implement the better long-term decisions to enhance operational efficiency for the overall supply chain.

The rest of paper is organized as follows. We review the related literature and highlight the research gaps and contributions of our study in Section 2. Section 3 first describes model notations and assumptions, then develop and analyze the single-period Stackelberg game model, and the multi-period dynamic Stackelberg game models are established and investigated in Section 4. Numerical simulation is conducted in Section 5 to explore complex dynamics of channel members' game strategies evolution process. Section 6 is proposed to examine the chain members' profits under different parameter conditions from a dynamic perspective. Section 7 outlines the conclusion, managerial insights and future research directions.

3. Problem description and model construction

Under the government's green subsidy and cap-and-trade regulation, we propose a dual-channel green supply chain comprising a manufacturer and an independent traditional retailer, in which the manufacturer employs low-carbon technology to produce green products, and distributes them through both direct and traditional retail sale channels. Meanwhile, to encourage the manufacturer to enhance emission abatement efforts, the government subsidies to the manufacturer based on the amount of emission reduction emitted. Meanwhile, the manufacturer usually charges more channel power and acts as the game leader, and the retailer is the game follower. Therefore, we use Stackelberg game theory to establish the single-period Stackelberg game and multi-period dynamic Stackelberg game model with consistent pricing strategy and inconsistent pricing strategies sequentially. The framework of the dual-channel green supply chain is illustrated below as shown in Fig. 1.

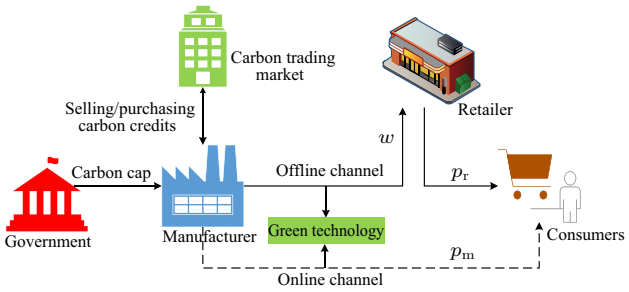


Fig. 1. The framework of dual-channel green supply chain.

3.1. Model notations

The model notation used through the paper and its definition are displayed in Table 1 for clarity.

3.2. Model assumption

To convenience the model construction, the following assumptions are proposed to develop mathematical models based on actual market competition.

Assumption 1 In line with previous research, we assume that both chain members are complete rationality in the single-period Stackelberg game models, while in multi-period Stackelberg game models, and the manufacturer is supposed to be the bounded rational agent, while the retailer determines her pricing decisions based on naïve expectation[20,35] (Zhang and Zhang, 2022; Zhang and Wang, 2018). Consequently, in each game period, the manufacturer first determines his strategy by considering the retailer's best response, after which the retailer decides her pricing strategy based on the information announced by the manufacturer.

Assumption 2 Without loss of generality, the demand function is a linear form function, which decreases with the product price and increases with the emission reduction rate of

the green product.[32,34,36] In practice, many companies pricing their products in online and offline channels are identical to mitigate channel conflicts, i.e., the consistent pricing strategy,[15] while several companies distribute their products with inconsistent pricing strategy in dual-channel settings.[21]

Assumption 3 The manufacturer engages in investing eco-friendly technology to reduce emissions. According to prior works,[12,25,37] the cost of green technology investment, denoted as I, is a quadratic function of the emission reduction rate e, and expressed by $I(e) = ke^2/2$, which is widely applied in supply chain management literature, the government provides subsidies to the manufacturer based on the emission reduction rate of the product, and the green subsidies for per unit emission reduction rate is denoted by λ. Hence, the total governmental green subsidies are $S = \lambda e(d_{\rm r} + d_{\rm m})$.

Assumption 4 The carbon quotas allocated to the manufacturer are determined by referencing his historical emission data. The manufacturer can purchase and sell carbon credits in the carbon trading market. Furthermore, assuming that the total carbon emission of the manufacturer is a linear function with respect to the initial carbon emissions of each product, then we have $E = (e_0 - e)(d_{\rm r} + d_{\rm m})$.[2,34]

Table 1. Notations.

Parameters	Description
$w^{\rm c}$	Wholesale price for per unit product under consistent pricing strategy
$p^{\rm c}$	Retail price/direct sale price for per unit product under consistent pricing strategy
$e^{\rm c}$	Emission reduction rate under consistent pricing strategy
w	Wholesale price for per unit product under inconsistent pricing strategy
$p_{\rm r}$	Retail price for per unit product under inconsistent pricing strategy
$p_{\rm m}$	Direct sale price for per unit product under inconsistent pricing strategy
e	Emission reduction rate under inconsistent pricing strategy
a	Market size, $a > 0$
ϕ	The customer loyalty degree to the retail channel, $0 < \phi < 1$
b	The sensitive coefficient of demand to the product price under consistent pricing strategy, $b > 0$
b_1	The sensitive coefficient of demand to the product price under inconsistent pricing strategy, $b_1 > 0$
b_2	The cross-sensitivity coefficient of demand to the competitor's product price under inconsistent pricing strategy, $0 < b_2 < b_1$
$\beta_{\rm r}$	The expansion effectiveness coefficient of emission reduction rate to the retail channel
$\beta_{\rm m}$	The expansion effectiveness coefficient of emission reduction rate to the direct sale channel
G	Carbon quotas of the manufacturer
c	Production cost per unit product
e_0	Initial emissions per unit product
h	Trading price per unit carbon emission
λ	Green subsidy for per unit emission reduction rate
k	The emission reduction cost coefficient
α_1	The adjustment speed of w^c
α_2	The adjustment speed of e^c
β_1	The adjustment speed of w
β_2	The adjustment speed of p
β_3	The adjustment speed of e
π_i	$i \in \{{\rm m}, {\rm r}\}$, which represents the profit of the manufacturer and retailer, respectively

In what follows, we first establish a single-period Stackelberg game model, then extend it into a multi-period dynamic Stackelberg game model with bounded rationality rule under a consistent pricing strategy, in which the retail price and direct sale price of the green product are identical. Based on the above conditions, the demand functions of traditional retail channel and direct sale channel under the consistent pricing strategy are given by

$$\begin{cases} d_{\rm r} = \phi a - bp^{\rm c} + \beta_{\rm r} e^{\rm c}, \\ d_{\rm m} = (1-\phi)a - bp^{\rm c} + \beta_{\rm m} e. \end{cases} \tag{1}$$

The profit function of the manufacturer and retailer is respectively given by

$$\pi_{\rm r} = (p^{\rm c} - w^{\rm c}) d_{\rm r}, \tag{2}$$

$$\begin{aligned} \pi_{\rm m} = {} & (p^{\rm c} - c + \lambda e^{\rm c}) d_{\rm m} + (w^{\rm c} - c + \lambda e^{\rm c}) d_{\rm r} \\ & - h((d_{\rm r} + d_{\rm m})(e_0 - e^{\rm c}) - G) - \frac{ke^2}{2}. \end{aligned} \tag{3}$$

Consequently, the optimization problem of the single-period Stackelberg game model is formulated as

Leader: $\pi_{\rm m}(w^{\rm c}, e^{\rm c}, p^{\rm c}) = (p^{\rm c} - c + \lambda e^{\rm c}) d_{\rm m} + (w^{\rm c} - c + \lambda e^{\rm c}) d_{\rm r} - h((d_{\rm r} + d_{\rm m})(e_0 - e^{\rm c}) - G) - \frac{k(e^{\rm c})^2}{2}$,

Follower: $\pi_{\rm r}(p^{\rm c}) = (p^{\rm c} - w^{\rm c}) d_{\rm r}$

$$\begin{cases} \pi_{\rm m} = (w^{\rm c}, e^{\rm c}, p^{\rm c}), \\ s.t. p^{\rm c} = arg\pi_{\rm r}(p^{\rm c}). \end{cases} \tag{4}$$

In Eq. (4), the first term of the manufacturer's profit function represents the revenue from direct sale channel, the second term represents profits from traditional retail channel, and the third part denotes the carbon trading revenue/cost, and the

last term signifies the manufacturer's emission reduction cost. Without loss of generality, the optimal equilibrium solution of the above optimization problem can be solved using the backward induction method.

Proposition 1 When

$$k > \frac{4b^2(h+\lambda)^2+\beta_{\rm m}^2-3\beta_{\rm r}^2+\beta_{\rm m}(8b(h+\lambda)+6\beta_{\rm r})}{6b},$$

there exists a unique optimal solution for the single-period Stackelberg game model. Due to the expression of it pretty complex, which is listed in Appendix A, and the proof of proposition 1 is displayed in Appendix B.

Thus far, we have derived the optimal strategy of the single-period Stackelberg game model under the assumption that both chain members are completely rational players. However, in reality, the decision-makers in the market can not achieve their optimal outcome through a one-shot game due to the complexity of the market environment, and the players only obtain partial market information and become bounded rational when determining their decisions.[38] Therefore, the decision process of them is usually multi-period dynamic game, which signifies the bounded rational players adjust their strategies in each game period according to the limited information.[39,40] Herein, we assume the manufacturer is a bounded rational agent who adjusts his channel price and emission reduction strategies by estimating marginal profit information, i.e., when the marginal profit associated with his decision variable is positive (negative) in the current period t, then the decision variable will be increased (decreased) in the next period $t+1$, such an adjustment method is called the gradient adjustment mechanism,[20,41] and the retailer is a naïve player who updates her price strategy based on the manufacturer's decision information. Therefore, the two-dimensional (2D) discrete dynamical adjustment system of the dual-channel green supply chain is formulated as

$$\begin{cases} w^{\rm c}(t+1) = w^{\rm c}(t)+\alpha_1 w^{\rm c}(t)\dfrac{\partial \pi_{\rm m}(t)}{\partial w^{\rm c}(t)}, \\ e^{\rm c}(t+1) = e^{\rm c}(t)+\alpha_2 e^{\rm c}(t)\dfrac{\partial \pi_{\rm m}(t)}{\partial e^{\rm c}(t)}, \\ p^{\rm c}(t+1) = \dfrac{bw^{\rm c}(t+1)+a\phi+e^{\rm c}(t+1)\beta_{\rm r}}{2b}, \end{cases} \tag{5}$$

where $\alpha_i > 0$, $(i=1,2)$ represents the adjustment speed of the wholesale price and emission reduction rate respectively. Moreover, $\partial\pi_{\rm m}/\partial w^{\rm c}$ and $\partial\pi_{\rm m}/\partial e^{\rm c}$ can be obtained from Appendix B. Submitting expressions of $\partial\pi_{\rm m}/\partial w^{\rm c}$ and $\partial\pi_{\rm m}/\partial e^{\rm c}$ into the system (5), then we have

$$\begin{cases} w^{\rm c}(t+1) = w^{\rm c}(t)+\alpha_1 w^{\rm c}(t)\left(\dfrac{1}{2}(a+b(2c+2e_0h-3w^{\rm c}-2e(h+\lambda))-a\phi+e\beta_{\rm m})\right), \\ e^{\rm c}(t+1) = e^{\rm c}(t)+\alpha_2 e^{\rm c}(t)\left(\dfrac{1}{2b}(F_1-2b(e^{\rm c}k+(h+\lambda)((bw^{\rm c}-a(1-\phi))))\right), \\ p^{\rm c}(t+1) = \dfrac{a\phi+bw^{\rm c}(t+1)+e^{\rm c}(t+1)\beta_{\rm r}}{2b}. \end{cases} \tag{6}$$

By imposing $w^{\rm c}(t+1)=w^{\rm c}(t)$ and $e^{\rm c}(t+1)=e^{\rm c}(t)$, we can get four long-term equilibrium solutions of the system (6), that is,

$$E_1=\left(0,0,\frac{a\phi}{2b}\right),\quad E_2=\left(0,F_2,\frac{a\phi+F_3}{2b}\right),\quad E_3=\left(\frac{a+2b(c+e_0h)-a\phi}{3b},0,\frac{a+2bc+2a\phi}{6b}\right),\quad E_4=\left(w^{\rm c^*},e^{\rm c^*},p^{\rm c^*}\right),$$

$$F_1=\beta_{\rm r}(a-2a\phi-e\beta_{\rm r})+\beta_{\rm m}(b(w+4e(h+\lambda)-2c-2e_0h)+a\phi+2e\beta_{\rm r}),$$

$$F_2=\frac{(a\phi-2b(c+e_0h))\beta_{\rm m}+a(2b(h+\lambda)(1-\phi)+\beta_{\rm r}(1-2\phi))}{2bk+\beta_{\rm r}^2-2\beta_{\rm m}(2b(h+\lambda)+\beta_{\rm r})},\quad F_3=\frac{\beta_{\rm r}((a\phi-2bc)\beta_{\rm m}+a(2b(h+\lambda)(1-\phi)+(1-2\phi)\beta_{\rm r}))}{2bk+\beta_{\rm r}^2-2\beta_{\rm m}(2b(h+\lambda)+\beta_{\rm r})}.$$

From an economic perspective, a meaningful equilibrium solution requires that all decision variables are positive, so it is obvious that E_1, E_2, and E_3 are the boundary solutions, while E_4 is the only Nash equilibrium point for the system (6).

Next, we center on investigating the local asymptotic stability of the Nash equilibrium solution, and the Jacobian matrix of the system (6) is calculated as follows:

$$J(w^{\rm c},e^{\rm c})=\begin{bmatrix} 1+\dfrac{\alpha_1 F_4}{2} & \dfrac{1}{2}w^{\rm c}\alpha_1(\beta_{\rm m}-2b(h+\lambda)) \\ \dfrac{e^{\rm c}\alpha_2(b\beta_{\rm m}-2b^2(h+\lambda))}{2b} & 1+\dfrac{\alpha_2 F_5}{2b} \end{bmatrix}, \tag{7}$$

$$\begin{aligned} F_4 &= a+2b(c+e_0h-3w^{\rm c}-e^{\rm c}(h+\lambda))-a\phi+e^{\rm c}\beta_{\rm m}, \\ F_5 &= \beta_{\rm r}(a-2a\phi-2e^{\rm c}\beta_{\rm r})+\beta_{\rm m}(b(w^{\rm c}+8e^{\rm c}(h+\lambda))+a\phi+4e^{\rm c}\beta_{\rm r}-2c-2e^{\rm c}h)-2b(2e^{\rm c}k+(h+\lambda)(bw^{\rm c}-a(1-\phi))). \end{aligned}$$

Proposition 2 E_1, E_2, and E_3 are the boundary solutions, and only E_4 are the unique equilibrium solution for the system (6).

The Jacobian matrix at the Nash equilibrium point E_4 is computed as

$$J(w^{c*},e^{c*})=\begin{bmatrix} 1+\frac{1}{2}\alpha_1 F_3\left(w^{c^*},e^{c^*}\right) & \frac{1}{2}w^{c^*}\alpha_1(\beta_m-2b(h+\lambda)) \\ \frac{e^*\alpha_2(b\beta_m-2b^2(h+\lambda))}{2b} & 1+\frac{1}{2b}\alpha_2 F_4\left(w^{c*},e^{c*}\right) \end{bmatrix}. \tag{8}$$

The characteristic equation of $J(w^*,e^*)$ can be expressed as

$$f(\lambda)=\lambda^2-T_r(\lambda)+\mathrm{Det}(\lambda), \tag{9}$$

where $T_r(\lambda)$ and $\mathrm{Det}(\lambda)$ represents the trace and determinant of Jacobian matrix, and

$$\begin{aligned} T_r(\lambda) &= 2+\frac{1}{2}\alpha_1 F_3\left(w^{c^*},e^{c^*}\right)+\frac{1}{2b}\alpha_2 F_4\left(w^{c^*},e^{c^*}\right), \\ \mathrm{Det}(\lambda) &= \left(1+\frac{1}{2}\alpha_1 F_3\left(w^{c^*},e^{c^*}\right)\right)\left(1+\frac{1}{2b}\alpha_2 F_4\left(w^{c^*},e^{c^*}\right)\right)-\left(\frac{1}{2}w^{c^*}\alpha_1(\beta_m-2b(h+\lambda))\right)\left(\frac{e^{c^*}\alpha_2(b\beta_m-2b^2(h+\lambda))}{2b}\right). \end{aligned}$$

In addition, the discriminant of the above characteristic equation is $\Delta=(T_r(\lambda))^2-4\mathrm{Det}(\lambda)$, and the characteristic equation has two real characteristic roots when $\Delta>0$, and a pair of conjugate characteristic roots when $\Delta<0$.

The sufficient and necessary conditions for the Nash equilibrium point is locally stable are given by

$$\begin{cases} f(-1)=1-T_r(\lambda)+\mathrm{Det}(\lambda)>0, \\ f(1)=1-T_r(\lambda)+\mathrm{Det}(\lambda)>0, \\ \mathrm{Det}(\lambda)-1<0. \end{cases} \tag{10}$$

When all the above inequalities are satisfied simultaneously, the eigenvalues of the Jacobian matrix are located within the unit circle, i.e., $|\lambda_i|<1$. Meanwhile, the Nash equilibrium point's stability domain in the plane of (α_1,α_2) is obtained. However, when the value of α_i $(i=1,2)$ falls outside the stable region, the Nash equilibrium point will lose its stability, leading to more complex behaviors, such as periodic cycles and chaos. More precisely, if there exists a real eigenvalue passes through -1, which leads to the first in equation in Eq. (10) is failed to meet, then a flip bifurcation appears. If there exists a real eigenvalue exceeds $+1$, which leads to the condition (ii) being invalid, then a fold or transcritical bifurcation comes up. Moreover, if the modulus of a complex eigenvalue is bigger than $+1$, which leads to the condition (iii) being invalid, then a Neimark–Sacker bifurcation takes place.[31]

Due to the computational complexity, it is quite difficult to directly seek the specific conditions of locally asymptotic stability for the Nash equilibrium point, we investigate the stability characteristics of the Nash equilibrium point by means of numerical simulations in the subsequent section.

4. Numerical simulation

In this section, we concentrate on exploring the dynamical evolution process of the chain members' long-run game strategies under different parameter conditions. The following data set is carefully chosen for the model parameters, i.e., $\alpha=300$, $\phi=0.4$, $b=3$, $\beta_r=1$, $\beta_m=0.8$, $c=15$, $e_0=10$, $G=200$, and the initiate values for the decision variables are $w(0)=30$ and $e(0)=2$.

Figure 2 illustrates the stability region of the Nash equilibrium point in terms of (α_1,α_2) under different parameter conditions. Figure 2(a) shows the changes in the stable regions of the Nash equilibrium point by assigning $\lambda=0.5,1.5,2.5$ sequentially when $h=1$. One can observe that with increase of λ, the value scope of α_1 is expended in some extent, whereas the value scope of α_2 narrows significantly, then the conclusion can be drawn that the larger green subsidy degree, the wider scope of the wholesale price adjustment speed and the narrower scope of the emission reduction rate adjustment speed. In addition, numerical experiments reveal that with increase of green subsidy degree, the system (6) is more sensitive to the adjustment speed of the emission reduction rate than that of wholesale price, so the manufacturer should more prudent to adjust the emission reduction rate of the product when the green subsidy degree is relatively high.

Figure 2(b) is presented to investigate the impact of h on the stable region of the Nash equilibrium point when h is assigned to 0.5, 1, 1.5 sequentially as $\lambda=1$. One can observe that with h increases, the stable regions of the Nash equilibrium point become smaller due to the value scopes of α_1 and α_2 are narrowed to some extent, which indicates that the high carbon trading price is not conducive to the stability of the Nash equilibrium point. Therefore, the manufacturer should slow down the adjustment speeds of wholesale price and emis-

sion reduction rate when the carbon trading price is relatively high.

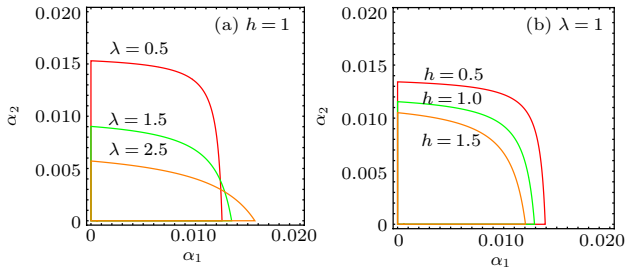


Fig. 2. The 2D stable region with varying λ and h.

As we know that the adjustment speed value of the manufacturer reflects the response speed of the manufacturer in adjusting his decision variables. From the above experiment results, the manufacturer should be careful to adjust the emission reduction rate of the product when the green subsidy for per unit emission reduction rate is relatively high, and the manufacturer should slowly adjust direct sell price and emission reduction rate of the product when the carbon trading price is relatively high.

Figures 3(a) and 3(b) present the dynamic evolution processes of price and emission reduction rate strategies of chain members with varying α_1 when $\alpha_2 = 0.005$. One can see that the trajectories of channel prices and emission reduction rate remain unchanged when $\alpha_1 \leq 0.01221$, as depicted in Fig. 3(a), which means the chain members' strategies stay at the Nash equilibrium point. However, as α_1 increases, the Nash equilibrium point gradually loses its stability, then the first bifurcation point occurs, and the system enters into a period-2 cycle, which indicates there exists two equilibrium solution for the channel members. After undergoing a series of period-doubling bifurcations, the system falls into the chaos region eventually, which implies the market becomes disorder and unpredictable associated with infinite number of equilibrium solutions. Under this condition, the channel member almost can't implement an appropriate business strategy to obtain more profits.

Figure 3(c) presents the largest Lyapunov exponent (LLE) diagram, which is widely applied to judge the dynamic motions of the chain members' strategy. The Lyapunov exponent can measure the chaotic state by measuring the convergence or separation rate of adjacent tracks. The larger the Lyapunov index is, the worse the local stability of the system is. More precisely, when the LLE is less than zero, it indicates that the dynamic system is in a stable state, including low and high periodic cycles, and the bifurcation points or quasi-period cycle take places when LLE equals to zero, while LLE greater than zero indicates that the system has entered a chaotic state.

In addition, power spectrum is an important tool in signal processing and physics to describe the distribution of signal power in the frequency domain, and it is an important method to study the system from bifurcation to chaos. Figure 3(d) displays the power spectrums of decision variables at $\alpha_1 = 0.016$. One can see that the power spectrums characteristic with white noise background and wide peaks within the limited range, which implies that the system behaviors chaotic under such condition, and periodic motion corresponds to peaks in the power spectrum, which there existing some periodic windows in chaotic range.

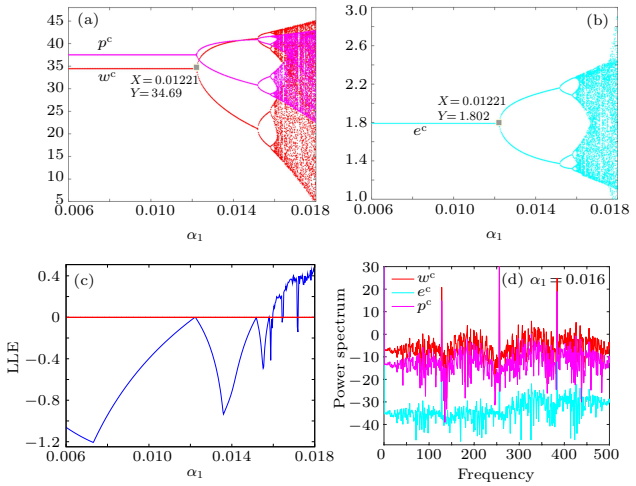


Fig. 3. Bifurcation diagram, LLEs and power spectrum with respect to $\alpha_2 = 0.005$.

Figure 4 proposes some chaotic attractors under different parameter conditions when fix $\alpha_2 = 0.005$, $h = 1$, and $\lambda = 1$. One can observe that there exist eight pieces of chaotic attractors as when $\alpha_1 = 0.016$, as shown in Fig. 4(a), and those eight chaotic attractors evolve into two chaotic attractors with a mild increase in α_1. As α_1 continues increasing, the two chaotic attractors evolve into a bigger chaotic attractor and its structure becomes more complex.

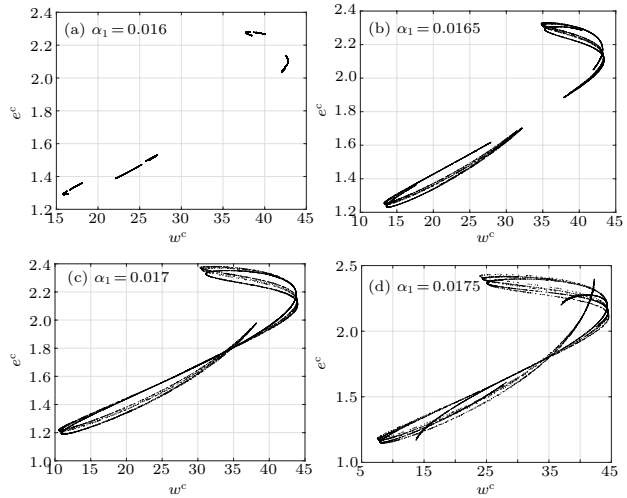


Fig. 4. Chaotic attractors with respect to $\alpha_2 = 0.005$, $h = 1$, and $\lambda = 1$.

The 2D bifurcation diagram is applied to explore the dynamical evolution process of the system (6) with varying two

vital parameters, as presented in Fig. 5, in which the red, blue, green, yellow, brown, pink, and cyan colors correspond to period-1, period-2, period-3, period-4, period-5, period-7, and period-8 cycles respectively. Besides, the black region indicates chaotic behavior, while the white area represents the infeasible region, signifying that one of the players withdraws from the market competition. Figures 5(a)–5(c) is drawn to examine the impacts of α_1 and α_2 on the system's complex dynamics under varying parameter conditions. By observing Figs. 5(a)–5(c), the system only experiences a series of period-doubling bifurcations and finally falls into chaotic region with increase in α_1 and α_2. Moreover, figure 5(d) is plotted to investigate the influence of the carbon trading price h and green subsidy degree λ on the system's complex dynamics as $\alpha_1 = \alpha_2 = 0.006$. When λ is small enough, the system always remains stable regardless of variation in h. Meanwhile, the relatively larger λ significantly destabilizes the system's stability when h is held constant.

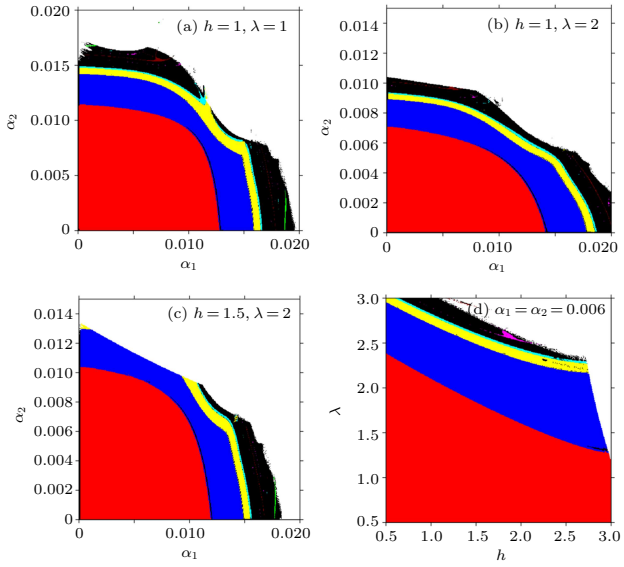


Fig. 5. The 2D bifurcation diagram with different parameter conditions.

From the numerical experiments conducted, one can conclude that the excessive adjustment speeds of wholesale price and emission reduction rate, the high green subsidy degree and carbon trading price have a destabilizing effect on the system's stability.

Figure 6 is plotted to examine the adjustment speeds of wholesale price and emission reduction rate on the profits of chain members. In Figs. 6(a) and 6(b), the profits of both the manufacturer and retailer reach their highest levels when α_1 and α_2 are small, which indicates that the system stays in its stability domain. When the values of α_1 and α_2 exceed a certain threshold, the system gets out of its stability domain, and more complex behaviors appear, such as bifurcation and chaos. Consequently, the profits of both the manufacturer and retailer decline and fluctuate violently.

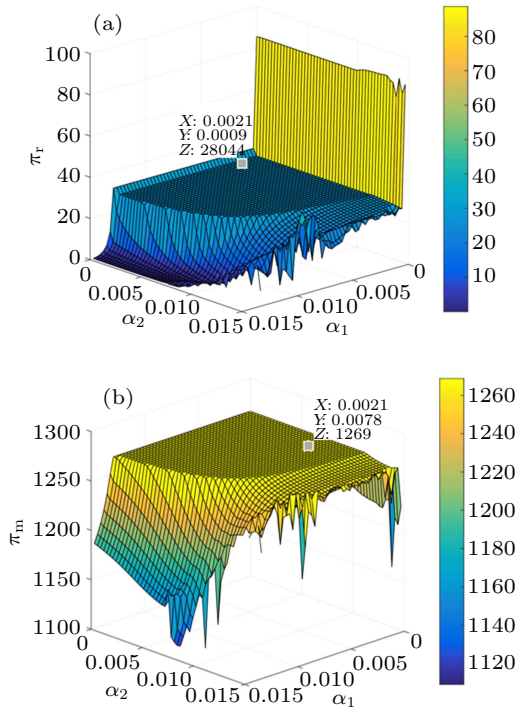


Fig. 6. Proft variations of the channel members with α_1 and α_2 when $h = 1, \lambda = 1$.

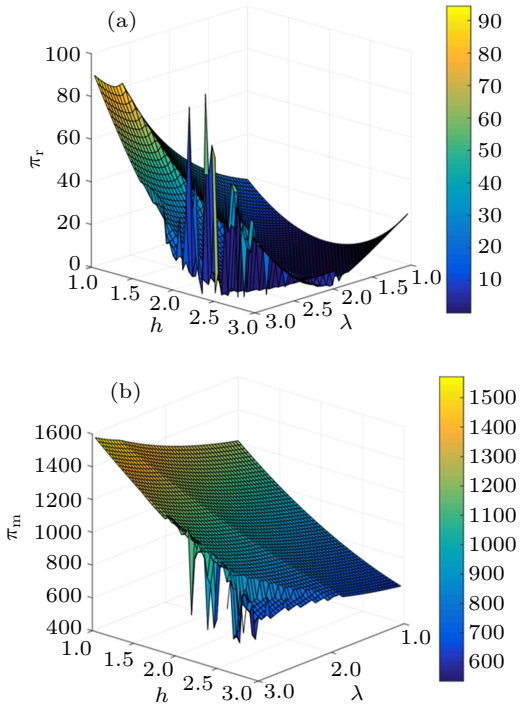


Fig. 7. Proft variations of channel members with h and λ when $\alpha_1 = \alpha_2 = 0.006$.

Figure 7 examines the impact of government's green subsidies and carbon trading price on the profits of chain members. Figure 7(a) presents the profit variations of the retailer with respect to h and λ. It is evident that the retailer achieves the highest profit when the carbon trading price is low and the green subsidy is high, and the retailer's profits change rapidly and irregular when the values of h and λ are sufficiently high, which represent the system's undergoes periodic cycles and

chaotic motions. Figure 7(b) explores the change trend of the manufacturer's profit with varying h and λ. It is observed that when λ is smaller than a threshold value, an increase in λ is disadvantage to the manufacturer's profits, while the manufacturer's profit is decreased with respect to λ and h, which indicates that the high carbon trading price and green subsidy degree are unfavorable for the manufacturer when the system rids out of its stability region.

From the above numerical simulations, we conclude that the manufacturer's adjustment speed has a significant impact on the complexity features of multi-period Stackelberg game models. In reality, chaos within economic and management systems is usually detrimental to decision-makers and decreases operational efficiency of the system. Therefore, as the game leader, the manufacturer should implement measures to control chaotic behaviors. Herein, we utilize the variable feedback control method to remove the chaotic behaviors appeared in Fig. 3(a). By utilizing this control method, the controlled system (7) can be expressed as

$$\begin{cases} w^{\mathrm{c}}(t+1) = (1-v)\left(w^{\mathrm{c}}(t) + \alpha_1 w^{\mathrm{c}}(t)\left(\frac{1}{2}\left(a + b\left(2c + 2e_0 h - 3w^{\mathrm{c}} - 2e^{\mathrm{c}}(h+\lambda)\right) - a\phi + e^{\mathrm{c}}\beta_{\mathrm{m}}\right)\right)\right) + v w^{\mathrm{c}}(t), \\ e^{\mathrm{c}}(t+1) = e^{\mathrm{c}}(t) + \alpha_2 e(t)\left(\frac{1}{2b}\left(F_1 - 2b\left(e^{\mathrm{c}}k + (h+\lambda)\left(bw^{\mathrm{c}} - a(1-\phi)\right)\right)\right)\right), \\ p^{\mathrm{c}}(t+1) = \dfrac{bw^{\mathrm{c}}(t+1) + a\phi + e^{\mathrm{c}}(t+1)\beta_{\mathrm{r}}}{2b}, \end{cases} \tag{11}$$

where v is controlling parameter, $0 < v < 1$, which can be regarded as the price control strategy of the government or learning ability of the decision makers. The chaos control processes with respect to v are proposed as described below.

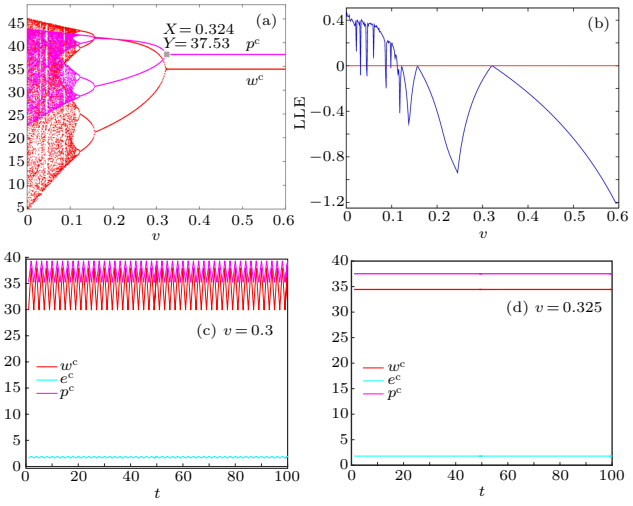


Fig. 8. Price trajectories, LLEs, and time series when $\alpha_1 = 0.018$ and $\alpha_2 = 0.005$.

As can be seen from Fig. 8(a), the trajectories of wholesale price and emission reduction rate with varying v from 0 to 0.6 is drawn with $\alpha_1 = 0.018$ and $\alpha_2 = 0.005$ (the system is in chaos region). One can observe that the price orbits of chain members is chaotic when v is in a small range. As v increases, the price orbits undergo a series of inverse period-doubling bifurcations and converge to the Nash equilibrium point at $v = 0.324$. Moreover, the corresponding LLE diagram is plotted in Fig. 8(b). Figures 8(c) and 8(d) show the time series of wholesale price and emission reduction rate when $v = 0.3$ and $v = 0.325$, respectively. The strategies of the chain members are stable when $v = 0.325$, which means that system (8) returns to the Nash equilibrium point again. Hence, the variable feedback control strategy can remove the chaotic behavior effectively.

5. Dual-channel green supply chain game models with inconsistent price strategy

5.1. Model construction and analysis

In this section, we sequentially develop the single-period and multi-period Stackelberg game models with inconsistent pricing strategy, in which the manufacturer's decision variables include the wholesale price w, the direct sale price p_{m} and the emission reduction rate e of the green product, and the retailer's decision variable is the retail price p_{r}. Based on the previous conditions, the demand function of the manufacturer and the retailer are expressed as follows:

$$\begin{cases} d_{\mathrm{r}} = \phi a - b_1 p_{\mathrm{r}} + b_2 p_{\mathrm{m}} + \beta_{\mathrm{r}} e, \\ d_{\mathrm{m}} = (1-\phi)a - b_1 p_{\mathrm{m}} + b_2 p_{\mathrm{r}} + \beta_{\mathrm{m}} e, \end{cases} \tag{12}$$

and the profit function of the manufacturer and retailer can be given as

$$\begin{aligned} \pi_{\mathrm{m}}(w, p_{\mathrm{m}}, e) &= (p_{\mathrm{m}} - c + \lambda e)d_{\mathrm{m}} + (w - c + \lambda e)d_{\mathrm{r}} \\ &\quad - h((d_{\mathrm{r}} + d_{\mathrm{m}})(e_0 - e) - G) - \frac{ke^2}{2}, \end{aligned} \tag{13}$$

$$\pi_{\mathrm{r}}(p_{\mathrm{r}}) = (p_{\mathrm{r}} - w)d_{\mathrm{r}}. \tag{14}$$

Consequently, the optimization problem of the single-period Stackelberg game model with inconsistent pricing strategy is formulated as

Leader: $\pi_{\mathrm{m}} = (p_{\mathrm{m}} - c + \lambda e)d_{\mathrm{m}} + (w - c + \lambda e)d_{\mathrm{r}} - h((d_{\mathrm{r}} + d_{\mathrm{m}})(e_0 - e) - G) - \frac{ke^2}{2}$,

Follower: $\pi_{\mathrm{r}} = (p_{\mathrm{r}} - w)\, d_{\mathrm{r}}$,

$$\begin{cases} \pi_{\mathrm{m}} = (w, p_{\mathrm{m}}, e, p_{\mathrm{r}}), \\ s.t. p_{\mathrm{r}} = \arg\max \pi_{\mathrm{r}}(p_{\mathrm{r}}). \end{cases} \tag{15}$$

Without loss of generality, we can use backward induction method to obtain the optimal solution of the above optimization problem.

Proposition 2 When $k > (F_4 + F_5)/4(b_1^3 - b_1 b_2^2)$ is satisfied, there exists a unique optimal solution for the single-period Stackelberg game model under inconsistent price strategy. Due to the expression of the optimal equilibrium solution is very complex, we list them in Appendix C.

In what follows, we focus on extending the above single-period Stackelberg game model into a multi-period dynamic Stackelberg game model considering the manufacturer is a bounded rational agent. Similar with the above section, we employ a gradient adjustment mechanism to formulate the manufacturer's dynamic adjustment strategy, which is formulated as

$$\begin{cases} w(t+1) = w(t) + \beta_1 w(t) \dfrac{\partial \pi_{\mathrm{m}}(t)}{\partial w(t)}, \\ p_{\mathrm{m}}(t+1) = p_{\mathrm{m}}(t) + \beta_2 p_{\mathrm{m}}(t) \dfrac{\partial \pi_{\mathrm{m}}(t)}{\partial p_{\mathrm{m}}(t)}, \\ e(t+1) = e(t) + \beta_3 e(t) \dfrac{\partial \pi_{\mathrm{m}}(t)}{\partial e(t)}, \end{cases} \tag{16}$$

where $\beta_i > 0$, $i \in (1,2,3)$ represents the manufacturer's adjustment speed parameters for the wholesale price, direct sale price, and emission reduction rate respectively, and the marginal profits associated with decision variables of the manufacturer are computed in Appendix C. Consequently, the discrete dynamical adjustment system of dual-channel green supply chain can be expressed as

$$\begin{cases} w(t+1) = w(t) + \beta_1 w(t) \dfrac{\partial \pi_{\mathrm{m}}(t)}{\partial w(t)}, \\ p_{\mathrm{m}}(t+1) = p_{\mathrm{m}}(t) + \beta_2 p_{\mathrm{m}}(t) \dfrac{\partial \pi_{\mathrm{m}}(t)}{\partial p_{\mathrm{m}}(t)}, \\ e(t+1) = e(t) + \beta_3 e(t) \dfrac{\partial \pi_{\mathrm{m}}(t)}{\partial e(t)}, \\ p_{\mathrm{r}}(t+1) = \dfrac{a\phi + w(t+1) b_1 + b_2 p_{\mathrm{m}}(t+1) + e(t+1)\beta_{\mathrm{r}}}{2b_1}. \end{cases} \tag{17}$$

By imposing $w(t+1) = w(t)$, $p_{\mathrm{m}}(t+1) = p_{\mathrm{m}}(t)$, and $e(t+1) = e(t)$, the system (17) reaches the long-term equilibrium state, and we can obtain eight equilibrium solutions. Moreover, there exist seven boundary equilibrium points are unstable points from economic perspective, and only one Nash equilibrium point for the system (17). Next, we concentrate on investigating the stability features of the Nash equilibrium point using the Jury criterion. To examine the local stability of the Nash equilibrium point, the Jacobian matrix of the system (16) is calculated as

$$J(w, p_{\mathrm{m}}, e) = \begin{bmatrix} 1+F_3 & w b_2 \beta_1 & F_4 \\ b_2 p_{\mathrm{m}} \beta_2 & 1+F_5 & F_6 \\ F_7 & F_8 & 1+F_9 \end{bmatrix}, \tag{18}$$

$$\begin{aligned}
F_3 &= \frac{1}{2}\beta_1(a\phi + (c + e_0 h - 4w - e(h+\lambda))b_1 + b_2(e(h+\lambda) + 2p_{\mathrm{m}} - c - e_0 h) + e\beta_{\mathrm{r}}), \\
F_4 &= \frac{1}{2} w \beta_1((h+\lambda)b_2 + \beta_{\mathrm{r}} - (h+\lambda)b_1), \\
F_5 &= \left(\frac{b_2^2}{b_1} - 2b_1\right) p_{\mathrm{m}} \beta_2 + \beta_2(a - a\phi - \frac{1}{2}(c + e_0 h - 2w - e(h+\lambda))b_2 + b_1(c + e_0 h - e(h+\lambda) - 2p_{\mathrm{m}}) \\
&\quad + e\beta_{\mathrm{m}} + \frac{b_2(a\phi + b_2(e(h+\lambda) + 2p_{\mathrm{m}}) + e\beta_{\mathrm{r-c-e_0h}})}{2b_1}, \\
F_6 &= \frac{p_{\mathrm{m}} \beta_2(b_1((h+\lambda)b_2 + 2\beta_{\mathrm{m}}) + b_2((h+\lambda)b_2 + \beta_{\mathrm{r}}) - 2(h+\lambda)b_1^2)}{2b_1}, \\
F_7 &= \frac{1}{2} e \beta_3((h+\lambda)b_2 + \beta_{\mathrm{r}} - (h+\lambda)b_1), \\
F_8 &= -\frac{e\beta_3(2hb_1^2 + 2\lambda b_1^2 - hb_1 b_2 - \lambda b_1 b_2 - hb_2^2 - \lambda b_2^2 - 2b_1\beta_{\mathrm{m}} - b_2\beta_{\mathrm{r}})}{2b_1}, \\
F_9 &= \frac{1}{2} e\beta_3\left(4(h+\lambda)\beta_{\mathrm{m}} + 2(h+\lambda)\beta_{\mathrm{r}} + \frac{2(h+\lambda)b_2\beta_{\mathrm{r}}}{b_1} - 2k\right) + \frac{1}{2}\beta_3(-2ek + a(h+\lambda)(2-\phi) \\
&\quad + b_2(h+\lambda)(w + p_{\mathrm{m}}) - b_1(h+\lambda)(w + 2p_{\mathrm{m}}) + 2(2e(h+\lambda) + p_{\mathrm{m}} - c - e_0 h)\beta_{\mathrm{m}} \\
&\quad + (w + 2e(h+\lambda) - c - e_0 h)\beta_{\mathrm{r}} + \frac{b_2((h+\lambda)(a\phi + b_2 p_{\mathrm{m}}) + (2e(h+\lambda) + p_{\mathrm{m}} - c - e_0 h)\beta_{\mathrm{r}})}{b_1}).
\end{aligned}$$

The characteristic polynomial equation of the dynamical system's Jacobian matrix can be expressed as

$$f(\lambda) = \lambda^3 + A_1\lambda^2 + A_2\lambda + A_3, \tag{19}$$

where

$$\begin{aligned}
A_1 &= F_4(1+F_5)F_7 + (1+F_3)F_6F_8 - (1+F_3)(1+F_5)(1+F_9) \\
&\quad - wb_2F_6F_7\beta_1 - b_2F_4F_8p_{\rm m}\beta_2 + wb_2^2(1+F_9)p_{\rm m}\beta_1\beta_2, \\
A_2 &= 3 - F_4F_7 - F_6F_8 + 2F_9 + F_5(2+F_9) \\
&\quad + F_3(2+F_5+F_9) - wb_2^2p_{\rm m}\beta_1\beta_2, \\
A_3 &= -3 - F_3 - F_5 - F_9.
\end{aligned}$$

The sufficient and necessary conditions to make sure the Jacobian matrix at the Nash equilibrium point should be satisfy the following Jury conditions[31,33,42]

$$\begin{cases}
f(1) = 1 + A + B + C, \\
f(-1) = -1 + A - B + C, \\
C^2 - 1 < 0, \\
(C-1)^2 > \left(AC - B^2\right)^2,
\end{cases} \tag{20}$$

When the above conditions are met simultaneously, we can guarantee all eigenvalues of $J(w, p_{\rm m}, e)$ will be located in the unit disk. Due to it is difficult to compute the specific expression of eigenvalues of the $J(w, p_{\rm m}, e)$, we utilize numerical simulations to study the Nash equilibrium point's stable region and dynamic strategies of the channel members under different parameter conditions.

5.2. Numerical simulation

This section we focus on studying the stability of the Nash equilibrium point and dynamic evolution process of chain members' strategies. We carefully chose data set for the parameters as follows: $\alpha = 300$, $\phi = 0.4$, $b_1 = 4$, $b_2 = 1.5$, $\beta_{\rm r} = 1$, $\beta_{\rm m} = 0.8$, $k = 100$, $e_0 = 10$, $G = 200$, and the initial values for the decision variables are $w(0) = 39$, $p(0) = 44$, and $e(0) = 2$. Remark that the data set employed satisfies the proposed inequalities in abovementioned section.

(i) The influence of λ and h on the stability of the Nash equilibrium point

Figure 9 describes the influence of the unit green subsidy λ and carbon trading price h on the stability of the Nash equilibrium point using the three-dimensional (3D) stable region defined by $(\beta_1, \beta_2, \beta_3)$. By comparing Figs. 9(a) and 9(b). One can see that the stable domain is significantly narrowed when λ increase from 0.5 to 1.5 as fix $h = 1$. By observing Figs. 9(c) and 9(d), the stable domain of the Nash equilibrium point is narrowed to some extent as h increases from 1 to 2 when $\lambda = 1$. Besides, with varying of λ and h, the value scopes of β_1 and β_2 change slightly, while the value scope of β_3 varies greatly. Moreover, the Nash equilibrium point's stable region is more sensitivity to the adjustment speed of the direct sale price.

From the above numerical simulations, we can conclude that the excessive large values of the green subsidy degree and carbon trading price have a destabilizing effect on the stability region of the Nash equilibrium point.

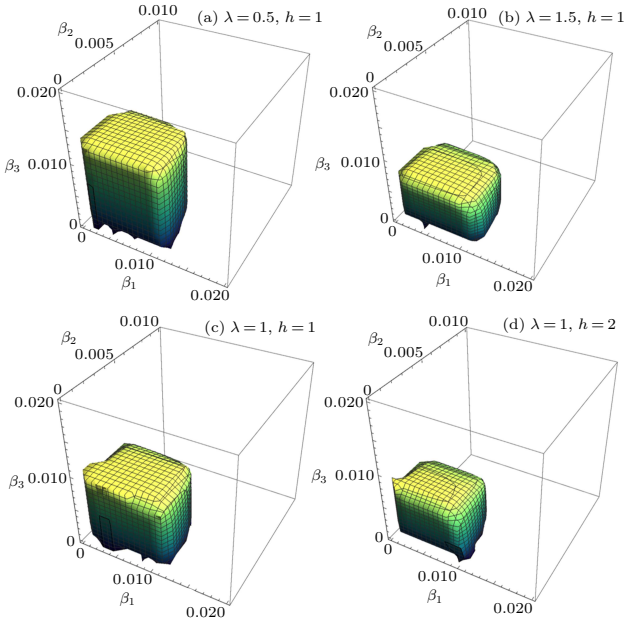


Fig. 9. The 3D stable regions of Nash equilibrium point with different values of λ and h.

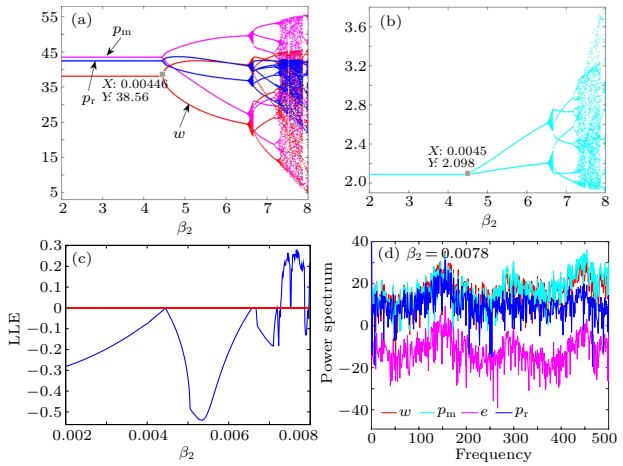


Fig. 10. Bifurcation diagram and the corresponding LLE diagram with respect to β_2 when $\beta_1 = 0.011$ and $\beta_3 = 0.003$.

Figure 10 is presented to investigate the impact of β_2 on the dynamical evolution of the channel members' strategy when $\beta_1 = 0.011$ and $\beta_3 = 0.003$. Figures 10(a) and 10(b) are plotted to investigate the adjustment speed of direct sale price β_2 on the dynamical evolution process of channel prices and emission reduction rate. One can see that the first bifurcation point appears at $\beta_2 = 0.00446$. As β_2 increases, the Nash equilibrium point of the system (10) loses its stability, and period-doubling bifurcation and Nermark–Sacker bifurcation occur. When β_2 exceeds the certain value, the system falls into chaotic region, resulting in unstable and unpredictable strategies. Figure 10(c) shows the corresponding LLE diagram, which can testify the dynamical evolution process of the decision variables depicted in Figs. 10(a) and 10(b). Moreover, the

power spectrum of the decision variables with $\beta_2 = 0.0078$, as shown in Fig. 10(d), which is continuous and remains within a limited range with white noise background, such features of the power spectrum implies that the system exhibits chaotic behavior under such a parameter condition.

The two-dimensional (2D) bifurcation diagram is one of the most effective tools for exploring the complex dynamics of a system, in which different period cycles are represented by different colors. Herein, we use the 2D bifurcation diagram to investigate the vital parameters on the system's dynamical evolution process. Figures 11(a)–11(c) are presented to explore the influence of two adjustment speed parameter as fix the other adjustment speed at 0.003, in which the red color, blue color, green color, yellow color, brown color, pink and cyan color represents period-1, -2, -3, -4, -5, -6, and -8 cycles, respectively. Besides, black color indicates the quasi-periodic cycle, while the white area denotes infeasible region of the system, which indicates that there exists one player withdraw from market competition.

As depicted in Fig. 11(a), with an increase of β_1 and β_2, the system gradually loses stability, thereby the period-doubling bifurcation first takes place, the system comes into a period-2 cycle. As β_1 and β_2 keep increasing, the system will go through a series of period-doubling bifurcation or Nermark–Sacker bifurcation, and enters the chaos region eventually. In Figs. 11(b) and 11(c), the system finally falls into chaos region after undergoing period-doubling bifurcations with varying the adjustment speed parameters of the manufacturer. Figure 11(d) is presented to study the effects of green subsidy degree and carbon trading price on the long-term strategy of the channel members. As λ and h increase, the system gets out of its stable domain and gets into chaotic motion. At the same time, the strategies of channel members tend to be disorder and irregular, it is difficult foe then to formulate suitable strategies to achieve optimal performance.

Based on the above experiments, one can see that the routes that from a steady state to the chaotic state may via a sequence of period-doubling bifurcation followed by Neimark–Sacker bifurcations. Furthermore, the excessive fast adjustment speeds, the excessive larger green subsidy degree and carbon trading price are not conducive to the system's stability.

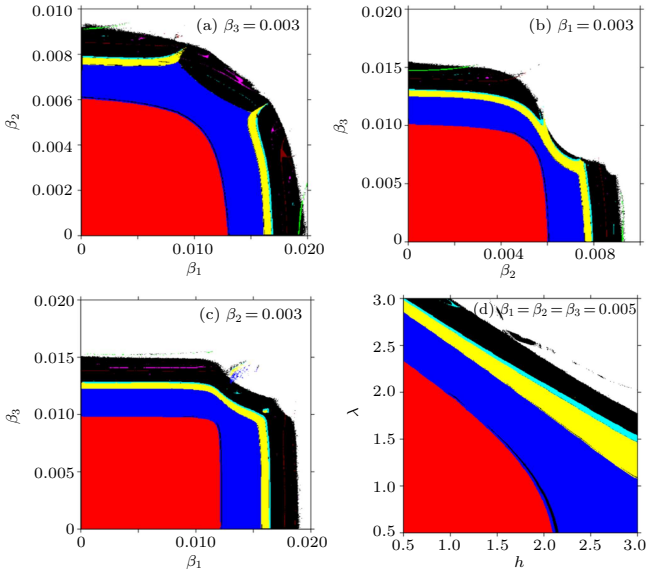


Fig. 11. The 2D bifurcation diagrams.

Figure 12 presents the attractor evolution process of system (16) for various values of β_1 as $\beta_2 = 0.0065$ and $\beta_3 = 0.003$. As shown in Fig. 12, the system (16) exhibits a period-6 cycle when $\beta_1 = 0.01215$. With a mild increase in β_1, two limit cycles appears, which indicates that the trajectories of channel members enter a quasi-periodic cycle, then the two limit cycles are broken out into a period-20 cycle, and evolve into twelve pieces of chaotic attractors as β_1 increases to 0.01306. After that, the above twelve pieces of chaotic attractors are contracted into two chaotic attractors, and eventually become a larger and more complicated chaotic attractor with fractal structure when $\beta_1 = 0.01397$.

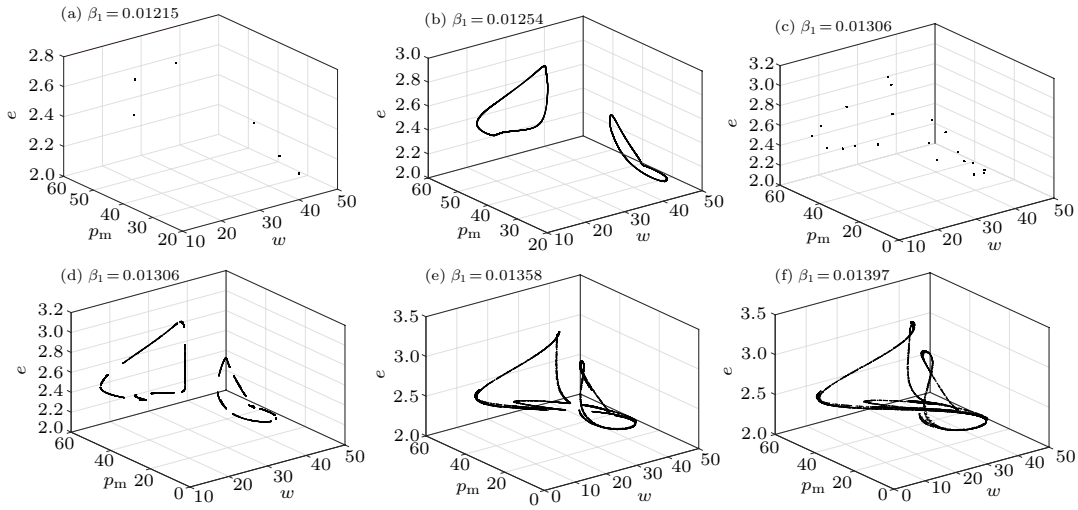


Fig. 12. Attractors with respect to β_1 when $\beta_2 = 0.0065$, $\beta_3 = 0.003$.

In what follows, we want to explore one of the important features of chaotic system, namely sensitivity dependence on initial conditions, also called "butterfly effect". By increasing $p_{\mathrm{m}}(0)=44$ to $p'_{\mathrm{m}}(0)=44.0001$, while keeping other initiate values for decision variables unchanged when $\beta_1=0.01358$, $\beta_2=0.0065$, and $\beta_3=0.003$, then the system is chaotic under such a situation. One can observe that the trajectories of channel prices and emission reduction rate as depicted in Fig. 13. The trajectory difference between two group of data sets is undistinguished at beginning, while after several iterations, the divergence between them is built rapidly and obviously. One can know that only a litter bit change in initial values, the dynamical evolution of the chaotic system can be different significantly, which reflects the randomness and unpredictability of chaotic motion.

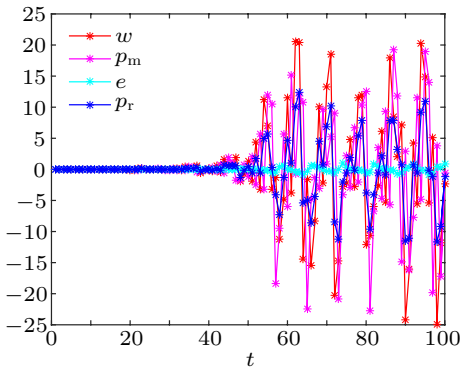


Fig. 13. The initial value sensitive dependency between $p_{\mathrm{m}}=44$ and $p'_{\mathrm{m}}=44.0001$ when $\beta_1=0.01358$, $\beta_2=0.0065$, $\beta_3=0.003$.

(ii) Impacts of key parameters on performance of chain members

Figures 14–16 are presented to study the essential parameters on profits of chain members with varying two adjustment speeds of the manufacturer as $\lambda=h=1$. By observing those graphs, it is obvious that the adjustment speeds in their small values, the profit of the manufacturer and retailer is 1748.96 and 95.6338 respectively, which indicates the system (16) stays at Nash equilibrium point. With increase of the adjustment speeds of manufacturer, the system (16) goes through a series of period-doubling bifurcations, which leads to most of chain members' profits are reduced to some degree. As the manufacturer's adjustment speeds continue increasing, the system eventually falls into chaotic motions, and most of channel members' profits are decreased and fluctuate violently. From the above numerical experiments, the system's steady state is benefit to the manufacturer, while the retailer can benefit from the period-doubling cycles of the system in most cases, and the system's chaotic behaviors are disadvantage to performance of both chain members.

Figure 17 shows the joint effect of λ and h on the profit variation of channel members. It can be found that both channel members' profits increase with λ and decrease with h. Moreover, when λ and h are larger enough, the channel members' profit varies significantly due to the system loses stability and more complex behaviors take place.

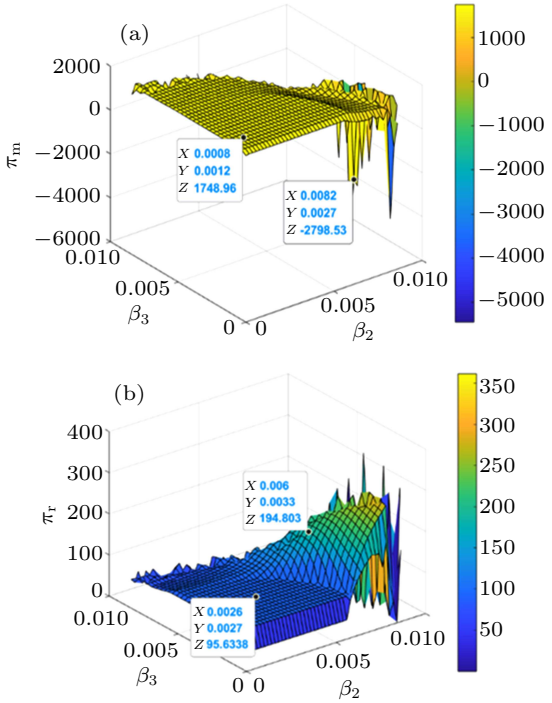


Fig. 14. The influence of β_2 and β_3 on profits of the chain members when $\beta_1=0.03$.

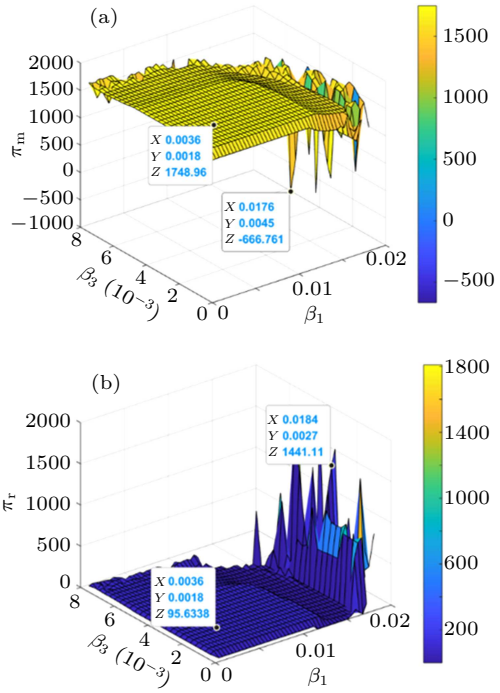


Fig. 15. The influence of β_1 and β_3 on profits of the chain members when $\beta_2=0.03$.

From the above numerical experiments, one can see that when the market stays in the stability region of the Nash equilibrium solution, the manufacturer can benefit from the stable system and achieve his highest profit level, while the retailer can gain more profit in some cases when the system goes through periodic cycles. However, the profit levels of them are

declined significantly when the market falls into chaos due to the channel member can't make an appropriate decision.

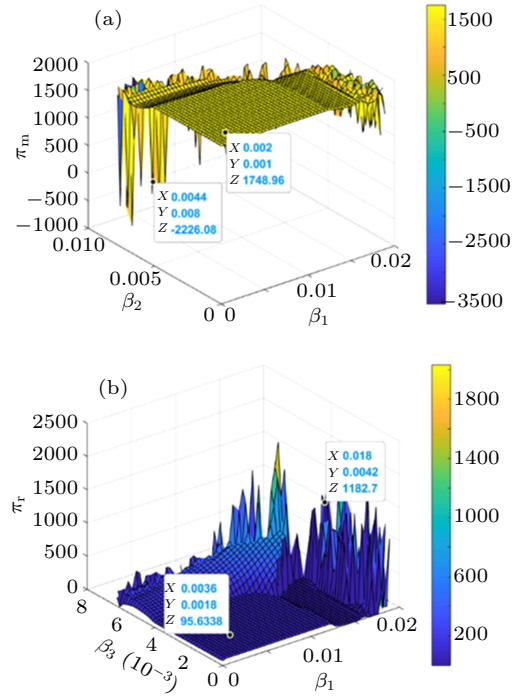


Fig. 16. The influence of β_1 and β_2 on profits of the chain members when $\beta_3 = 0.03$.

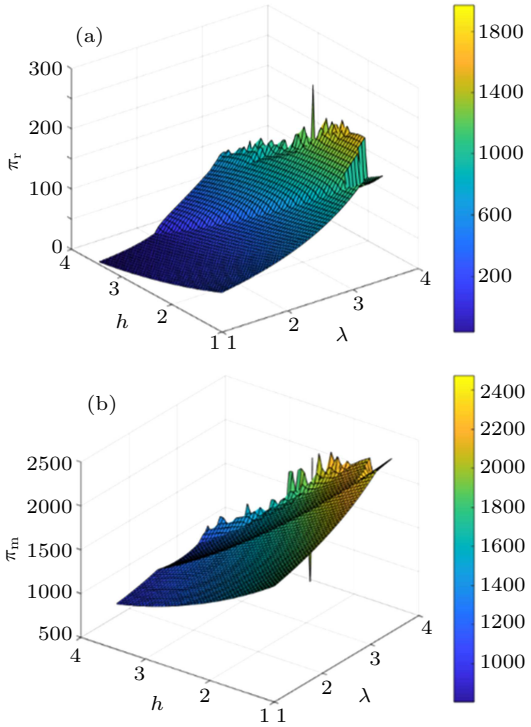


Fig. 17. The influence of λ and h on profits of the chain members when $\beta_1 = \beta_2 = \beta_3 = 0.005$.

5.3. Chaos control

In this subsection, in order to eliminate the system's chaotic behaviors, we use the delay feedback control method to remove the system chaos when $\beta_1 = 0.011$, $\beta_2 = 0.0078$, and $\beta_3 = 0.003$, and the system is chaotic under such a parameter condition. To implement this control approach, we need to add a control term in the first equation of the system (20), then the controlled system can be expressed as

$$\begin{cases} w(t+1) = w(t) + \beta_1 w(t)\dfrac{\partial \pi_m(t)}{\partial w(t)} + u\left(w(t+1) - w(t)\right), \\ p_m(t+1) = p_m(t) + \beta_2 p_m(t)\dfrac{\partial \pi_m(t)}{\partial p_m(t)}, \\ e(t+1) = e(t) + \beta_3 e(t)\dfrac{\partial \pi_m(t)}{\partial e(t)}, \\ p_r(t+1) = \dfrac{a\phi + w(t+1)b_1 + b_2 p_m(t+1) + e(t+1)\beta_r}{2b_1}, \end{cases} \tag{21}$$

where u is the controlling factor, and $u > 0$. The dynamical evolution process of the controlled system (21) is presented as follows:

In Fig. 18(a), the trajectories of channel prices are chaotic when u is within a small range. As u increases, the price orbits undergo a sequence of inverse period-doubling bifurcation and return to the Nash equilibrium point when $u = 0.762$, which indicates that the system has gotten out of the chaos region. The corresponding LLE diagram is presented as shown in Fig. 18(b). Figure 19 describes the time series of channel prices associated with different values of u. One can see that the channel prices' orbits bifurcate into a period-2 cycle when $u = 0.75$, and gradually converge to the Nash equilibrium point at $u = 0.77$, which demonstrates that the chain members' strategies return to the Nash equilibrium point once again.

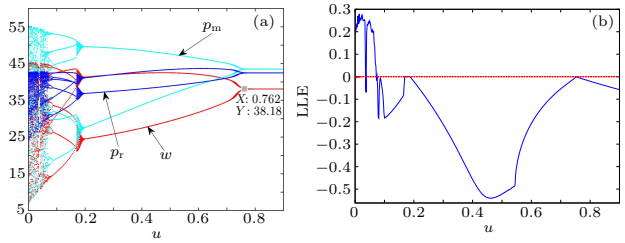


Fig. 18. The controlled channel price orbits with u varying from 0 to 0.9.

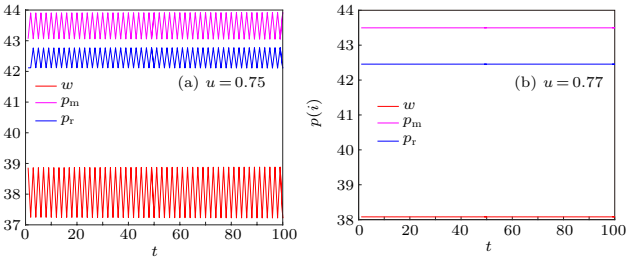


Fig. 19. Time series of the channel price orbits with different values of u.

6. Conclusions, managerial insights, and future research directions

6.1. Conclusions

In this study, we propose a dual-channel green supply chain that takes into account consumer environmental aware-

ness, the governmental green subsidy and cap-and-trade policies. The single-period Stackelberg and multi-period Stackelberg game models are established with consistent and inconsistent price strategy respectively. The optimal equilibrium solution is derived by means of backward induction approach for the single-period Stackelberg game models. Furthermore, the single-period Stackelberg game models are extended to the multi-period Stackelberg game models with gradient adjustment mechanism. Moreover, the existence and local stability of the equilibrium points are examined, and the chain members' long-run strategies and its complex dynamics are investigated by numerical simulation and chaos theory. The results reveal that in the single-period Stackelberg game model, the government's green subsidy is benefit to improving the chain members' performance while the high carbon trading price is disadvantage to the chain members. Meanwhile, the excessive high adjustment speeds of channel prices and emission reduction rate, green subsidy degree and carbon trading price have a destabilizing effect on the system's stability. As a result, the more complex behaviors take place, including different types of bifurcations and chaos. The manufacturer achieves his highest profit when the system stays in the stability region of the Nash equilibrium point, while the retailer can benefit from the period-doubling bifurcations, and both chain members' performance is declined as the system behaviors chaotic. In addition, the variable feedback control and delay feedback control method can remove the system chaos effectively when the value of the control parameter is chosen properly.

6.2. Managerial insights

(i) In practice, many governments share with the manufacturers' emission reduction cost to stimulate them to makes more efforts in emission reduction. Although the government's green subsidies are conducive to reducing carbon emissions, however, when the green subsidy degree is excessive high, the supply chain system is more easily loses it stability. Therefore, when the government enacts the green subsidy policy, it is necessary to implement a suitable green subsidy level according to different types of industries, which is advantage to make a trade-off between the emission abatement reduction and the stability of the supply chain system.

(ii) Cap-and-trade regulation has a great impact on the chain members' optimal equilibrium solution and performance, especially the carbon trading price can exert a significant influence on complex dynamics of the chain members' long-term strategy. Due to the relatively high carbon trading price is disadvantage to the system's stability, the government should take some measures to adjust it in a proper range to prevent the supply chain system from entering the period cycles and chaotic motions. Doing this can entail the chain members to charge more chance to implement a better long-run dynamic strategy.

(iii) As the game leader, the bounded rational manufacturer's adjustment strategy has a substantial impact on the dynamical evolution of pricing and emission reduction decisions in dual-channel supply chain. The overfast adjustment speed is detrimental to the system's stability and performance of chain members, which requires the manufacturer to control his adjustment speed in an appropriate range, so as to the manufacturer's adjustment strategy in each game period more reasonable, otherwise, the profits of chain members will be declined when the system behaviors periodic and chaotic.

6.3. Future research directions

Our study has some limitations and can be further studied from the following aspects: First, our work does not consider the uncertain factors of dual-channel supply chain, such as demand uncertainty, supply uncertainty, and so on, and considering these uncertain factors can make research closer to reality; Second, the behavioral preferences of chain members have a great impact on their decision-making, such as risk aversion and fairness concern behaviors, *etc*. Hence, it is necessary to study the game models by integrating abovementioned preference behaviors; Third, investigating the short-term and long-term decisions of the dual-channel supply chain game models under different government green subsidies and carbon quota allocation modes would be an interesting topic.

Appendix A: Derivation of the optimal solution of the single-period Stackelberg game model with consistent pricing strategy

We first compute the first-order condition of $\pi_{\mathrm{r}}^{\mathrm{c}}$ with respect to p^{c}, that is, $\frac{\partial \pi_{\mathrm{r}}^{\mathrm{c}}}{\partial p^{\mathrm{c}}} = -2bp^{\mathrm{c}} + bw^{\mathrm{c}} + a\phi + e^{\mathrm{c}}\beta_{\mathrm{r}}$, and the corresponding second-order condition is $\frac{\partial^2 \pi_{\mathrm{r}}^{\mathrm{c}}}{\partial (p^{\mathrm{c}})^2} = -2b < 0$, which indicates $\pi_{\mathrm{r}}^{\mathrm{c}}$ is concave at p^{c}. Hence, the retailer's best response function can be easily calculated as $p^{\mathrm{c}} = \frac{bw^{\mathrm{c}} + a\phi + e^{\mathrm{c}}\beta_{\mathrm{r}}}{2b}$. Plugging p^{c} into the manufacturer's profit function $\pi_{\mathrm{m}}^{\mathrm{c}}$, and seek the first-order partial derivatives of $\pi_{\mathrm{m}}^{\mathrm{c}}$ with respect to w^{c} and e^{c} respectively, which is given by

$$\begin{cases} \dfrac{\partial \pi_{\mathrm{m}}^{\mathrm{c}}}{\partial w^{\mathrm{c}}} = \dfrac{1}{2}(a + b(2c + 2e_0 h - 3w^{\mathrm{c}} - 2e^{\mathrm{c}}(h+\lambda)) - a\phi + e^{\mathrm{c}}\beta_{\mathrm{m}}), \\ \dfrac{\partial \pi_{\mathrm{m}}^{\mathrm{c}}}{\partial e^{\mathrm{c}}} = \dfrac{1}{2b}(-2b(e^{\mathrm{c}}k + (h+\lambda)(bw^{\mathrm{c}} + a(\phi - 1))) + F_1), \end{cases} \tag{A1}$$

$$F_1=\beta_{\rm r}(a-2a\phi-e^{\rm c}\beta_{\rm r})+\beta_{\rm m}(b(w^{\rm c}+4e(h+\lambda)-2c-2e_0h)+a\phi+2e^{\rm c}\beta_{\rm r}).$$

Furthermore, the second-order partial derivatives of $\pi_{\rm m}^{\rm c}$ with respect to $w^{\rm c}$ and $e^{\rm c}$ can be computed respectively, and the Hessian matrix of $\pi_{\rm m}^{\rm c}$ is expressed as

$$H_{\rm m}^{\rm c}=\begin{bmatrix} -\dfrac{3b}{2} & \dfrac{1}{2}(\beta_{\rm m}-2b(h+\lambda)) \\ \dfrac{1}{2}(\beta_{\rm m}-2b(h+\lambda)) & \dfrac{2\beta_{\rm m}(2b(h+\lambda)+\beta_{\rm r})-2bk-\beta_{\rm r}^2}{2b} \end{bmatrix}. \tag{A2}$$

By observing the above matrix, it is obvious that the first-order principal minor of $H_{\rm m1}^{\rm c}$ is negative, and the second-order principal minor of $H_{\rm m}^{\rm c}$ is calculated as

$$H_{\rm m2}^{\rm c}=\frac{1}{4}(2b(3k-2b(h+\lambda)^2)-\beta_{\rm m}(8b(h+\lambda)+\beta_{\rm m})-6\beta_{\rm m}\beta_{\rm r}+3\beta_{\rm r}^2). \tag{A3}$$

To guarantee $\pi_{\rm m}^{\rm c}$ is jointly concave at $w^{\rm c}$ and $e^{\rm c}$ simultaneously, the second-order principal minor $H_{\rm m}^2$ should be larger than zero, it is requires that $k>\dfrac{4b^2(h+\lambda)^2+\beta_{\rm m}^2-3\beta_{\rm r}^2+\beta_{\rm m}(8b(h+\lambda)+6\beta_{\rm r})}{6b}$. Then, the optimal solution of the manufacturer is derived by imposing $\partial\pi_{\rm m}^{\rm c}/\partial w^{\rm c}=\partial\pi_{\rm m}^{\rm c}/\partial e^{\rm c}=0$. By substituting $w^{\rm c}$ and $e^{\rm c}$ into $p^{\rm c}$, the retailer's optimal retailing price is realized. Thus far, the optimal equilibrium solution of the single-period Stackelberg game model with consistent pricing strategy is achieved

$$\begin{aligned}
w^{\rm c*} &= [-2b(2b(c+e_0h)k+a(2b(h+\lambda)^2-k)(\phi-1))+(2b(c+e_0h)-a\phi)\beta_{\rm m}^2-2ab(h+\lambda)(2\phi-1)\beta_{\rm r} \\
&\quad +(a(\phi-1)-2b(c+e_0h))\beta_{\rm r}^2+\beta_{\rm m}(2b(a+2b(c+e_0h))(h+\lambda)+(a+4b(c+e_0h))\beta_{\rm r})] \\
&\quad \times[b(2b(2b(h+\lambda)^2-3k)+\beta_{\rm m}^2-3\beta_{\rm r}^2+\beta_{\rm m}(8b(h+\lambda)+6\beta_{\rm r}))]^{-1}, \\
e^{\rm c*} &= [(4b(h+\lambda)(b(c+e_0h)+a(\phi-1))-(a-4b(c+e_0h)+2a\phi)\beta_{\rm m}+3a(2\phi-1)\beta_{\rm r})] \\
&\quad \times[2b(2b(h+\lambda)^2-3k)+\beta_{\rm m}^2-3\beta_{\rm r}^2+\beta_{\rm m}(8b(h+\lambda)+6\beta_{\rm r})]^{-1}, \\
p^{\rm c*} &= [(b(2ab(h+\lambda)^2-2bk(c+e_0h)-ak(1+2\phi)+(h+\lambda)(a+2b(c+e_0h)+4a\phi)\beta_{\rm m}+(c+e_0h)\beta_{\rm m}^2) \\
&\quad +(b(2b(c+e_0h)-a)(h+\lambda)+2(2b(c+e_0h)+a\phi)\beta_{\rm m})\beta_{\rm r}+(2a(\phi-1)-b(c+e_0h))\beta_{\rm r}^2)] \\
&\quad \times[b(2b(2b(h+\lambda)^2-3k)+\beta_{\rm m}^2-3\beta_{\rm r}^2+\beta_{\rm m}(8b(h+\lambda)+6\beta_{\rm r}))]^{-1}
\end{aligned}$$

Appendix B

Seeking the optimal solution of the single-period Stackelberg game model with an inconsistent pricing strategy.

We first take the first-order condition of $\pi_{\rm r}$ with respect to $p_{\rm r}$, i.e., $\dfrac{\partial\pi_{\rm r}}{\partial p_{\rm r}}=a\phi+b_2p_{\rm m}+b_1(w-2p_{\rm r})+\beta_{\rm r}e$, and the corresponding second-order condition is computed as $\dfrac{\partial^2\pi_{\rm r}}{\partial(p_{\rm r})^2}=-2b_1<0$, which indicates that $\pi_{\rm r}$ is concave at $p_{\rm r}$. Then, the retailer's best response function can be easily computed as $p_{\rm r}=\dfrac{a\phi+wb_1+b_2p_{\rm m}+e\beta_{\rm r}}{2b_1}$. Next, substituting $p_{\rm r}$ into the manufacturer's profit function $\pi_{\rm m}$, and taking the first-order condition of $\pi_{\rm m}$ with respect to w, $p_{\rm m}$, and e respectively, then we have

$$\begin{aligned}
\frac{\partial\pi_{\rm m}}{\partial w} &= \frac{1}{2}(a\phi+(c+e_0h-2w-e(h+\lambda))b_1+b_2(e(h+\lambda)+2p_{\rm m}-c-e_0h)+e\beta_{\rm r}), \\
\frac{\partial\pi_{\rm m}}{\partial p_{\rm m}} &= a-a\phi-\frac{1}{2}(c+e_0h-2w-e(h+\lambda))b_2+b_1(c+e_0h-e(h+\lambda)-2p_{\rm m}) \\
&\quad +e\beta_{\rm m}+\frac{b_2(a\phi+b_2(e(h+\lambda)+2p_{\rm m}-c-e_0h)+e\beta_{\rm r})}{2b_1}, \\
\frac{\partial\pi_{\rm m}}{\partial e} &= \frac{1}{2}((h+\lambda)b_2(w+p_{\rm m})-2ek-a(h+\lambda)(\phi-2)-(h+\lambda)b_1(w+2p_{\rm m})+2(2e(h+\lambda)+p_{\rm m}-c-e_0h)\beta_{\rm m} \\
&\quad +(w+2e(h+\lambda)-c-e_0h)\beta_{\rm r}+\frac{b_2((h+\lambda)(a\phi+b_2p_{\rm m})+(2e(h+\lambda)+p_{\rm m}-c-e_0h)\beta_{\rm r})}{b_1}).
\end{aligned}$$

To check the concave of $\pi_{\rm m}$ with respect to w, $p_{\rm m}$, e, the second-order and mixed second-order partial derivatives associated with $\pi_{\rm m}$ are calculated, and the Hession matrix of $\pi_{\rm m}$ with inconsistent pricing strategy can be expressed as

$$H_{\mathrm{m}}=\begin{bmatrix} -b_1 & b_2 & F_{10} \\ b_2 & -2b_1+\dfrac{b_2^2}{b_1} & F_{11} \\ F_{10} & F_{11} & (h+\lambda)(2\beta_{\mathrm{m}}+\left(1+\dfrac{b_2}{b_1}\right)\beta_{\mathrm{r}})-k \end{bmatrix}. \tag{B1}$$

By observing the above matrix, it is obvious that the first-order principal minor of H_{m1} is negative, i.e., $H_{\mathrm{m1}}=-b_1<0$, and the second-order principal minor $H_{\mathrm{m2}}=2b_1^2-2b_2^2>0$, and the third-order principal minor of H_{m} is

$$\begin{aligned} H_{\mathrm{m3}} &= F_{11}(F_{11}b_1+F_{10}b_2)+F_{10}\left(2F_{10}b_1+F_{11}b_2-\frac{F_{10}b_2^2}{b_1}\right) \\ &\quad +2(b_1^2-b_2^2)((h+\lambda)\left(2\beta_{\mathrm{m}}+(1+\frac{b_2}{b_1})\beta_{\mathrm{r}}-)\right), \end{aligned}$$

where

$$\begin{aligned} F_{10} &= \frac{1}{2}((h+\lambda)b_2+\beta_{\mathrm{r}}-(h+\lambda)b_1), \\ F_{11} &= \frac{1}{2}\left((h+\lambda)b_2+2\beta_{\mathrm{m}}+\frac{b_2((h+\lambda)b_2+\beta_{\mathrm{r}})}{b_1}\right. \\ &\quad \left.-2(h+\lambda)b_1\right). \end{aligned}$$

To guarantee π_{m} is strictly concave in w, p_{m}, and e simultaneously, $|H_{\mathrm{m3}}|$ should be larger than zero, then we have $k>\frac{F_{12}+F_{13}}{4(b_1^3-b_1b_2^2)}$, where

$$\begin{aligned} F_{12} &= 3(h+\lambda)^2b_1^4+2b_1b_2((h+\lambda)b_2-2\beta_{\mathrm{m}})((h+\lambda)b_2-\beta_{\mathrm{r}}) \\ &\quad -2(h+\lambda)b_1^3((h+\lambda)b_2-2\beta_{\mathrm{m}}-\beta_{\mathrm{r}}), \\ F_{13} &= b_2^2(\beta_{\mathrm{r}}-(h+\lambda)b_2)^2 \\ &\quad +b_1^2(2\beta_{\mathrm{m}}^2+2(h+\lambda)b_2\beta_{\mathrm{r}}+\beta_{\mathrm{r}}^2-4(h+\lambda)^2b_2^2). \end{aligned}$$

In what follows, by imposing $\partial\pi_{\mathrm{m}}/\partial w=\partial\pi_{\mathrm{m}}/\partial p_{\mathrm{m}}=\partial\pi_{\mathrm{m}}/\partial e=0$ simultaneously, we can obtain the optimal equilibrium strategy of the manufacturer, in turn, putting w^*, p_{m}^*, and e^* into the best response function of the retailer, then the optimal retail price p_{r}^* is realized. Thus far, the optimal solution of the single-period Stackelberg game model with inconsistent pricing strategy is derived. However, since the expressions of the optimal equilibrium solution is very complex, we omitted them here.

Acknowledgements

Project supported by the General Projects of Philosophy and Social Science Research in Jiangsu Province Universities (Grant No. 2024SJYB1101), the National Youth Fund Guidance Project of Jiangsu University of Science and Technology (Zhangjiagang Campus), the Special Project for Cultivating Leading Talents in Philosophy and Social Science Planning of Zhejiang Province, China (Grant No. 22YJRC14ZD), the Shanghai Pujiang Program (Grant No. 2021PJC066), and the National Natural Science Foundation of China (Grant No. 72302142).

References

[1] Cai J H and Jiang F Y 2023 *Int. J. Prod. Econ.* **264** 108964
[2] Lyu R X, Zhang C H, Li Z T and Li Y T 2022 *Comput. Ind. Eng.* **163** 107769
[3] Hu X, Yang Z J, Sun J and Zhang Y L 2020 *J. Clean. Prod.* **243** 118606
[4] Zou H, Qin J and Zheng H 2023 *J. Clean. Prod.* **407** 137107
[5] Ma J H and Wang Z X 2022 *Appl. Math. Model* **111** 610
[6] Xu S, Govindan K, Wang W R and Yang W T 2024 *Int. J. Prod. Econ.* **271** 109199
[7] Li Z M, Pan Y C, Yang W Ma J and Zhou M 2021 *Energy. Econ.* **101** 105426
[8] Cao K Y, Xu X P, Wu Q and Zhang Q P 2017 *J. Clean. Prod.* **167** 505
[9] Jauhari W A, Ramadhany S C N, Rosyidi C N, Mishra U and Hishamuddin H 2023 *J. Clean. Prod.* **425** 138897
[10] Zhu C, Xi X and Goh M 2024 *J. Environ. Manage.* **358** 120913
[11] Song H H, Wang Y, Mao X Y and Wang C Y 2024 *Expert. Syst. Appl.* **237** 121606
[12] Bian J S, Zhang G Q and Zhou G H 2020 *Eur. J. Oper. Res.* **287** 832
[13] Xu G Y, Dan B, Zhang X M and Liu C 2014 *Int. J. Prod. Econ.* **147** 171
[14] Ghosh S K, Seikh M R and Chakrabortty M 2020 *Comput. Ind. Eng.* **149** 106765
[15] Li B, Zhu M Y, Jiang Y S and Li Z H 2016 *J. Clean. Prod.* **112** 2029
[16] Ma J H, Hou Y M, Wang Z X and Yang W H 2021 *Energy. Policy* **148** 111919
[17] Yang R, Tang W S and Zhang J X 2021 *Eur. J. Oper. Res.* **289** 553
[18] Meng Q, Li M W, Liu W Y, Li Z and Zhang J 2021 *Sustain. Prod. Consum.* **26** 1021
[19] Barman A, De P K, Chakraborty A K, Lim C P and Das R 2023 *Math. Comput. Simul.* **204** 401
[20] Zaefarian T, Fander A and Yaghoubi S 2024 *Ann. Oper. Res.* **336** 1965
[21] Barman H, Pervin M, Roy S K and Weber G W 2023 *Int. J. Syst. Sci.Oper. Logist.* **10:1** 2242770
[22] Yang, M 2023 *Comput. Ind. Eng.* **177** 109036
[23] Yang M Zhang T and Zhang Y H 2022 *Environ. Sci. Pollut. Res.* **29** 28208
[24] Zhang S Y, Wang C X, Yu C and Ren Y J 2019 *Comput. Ind. Eng.* **134** 27
[25] Li J, Wang H Y, Shi V and Sun Q 2024 *Eur. J. Oper. Res.* **1** 131
[26] Chai Q F, Sun M Y, Lai K H and Xiao Z D 2023 *Comput. Ind. Eng.* **178** 109126
[27] Ma J H, Si F S, Zhang Q and Hui J 2023 *Int. J. Prod. Res.* **61** 6675
[28] Ma J H, Tian Y, Xu T T, Koivumäki T and Xu Y Q 2022 *Chaos, Solitons and Fractals* **160** 112131
[29] Ma J H and Xie L 2016 *Nonlinear Dyn.* **83** 1379
[30] Zhao L W, Jin S and Jiang H Y 2022 *Chaos, Solitons and Fractals* **164** 112492
[31] Zhang Y H and Zhang T 2023 *Int. J. Bifur. Chaos* **33** 2350099
[32] Zhang F and Wang C 2018 *Appl. Math. Model.* **54** 722
[33] Zhu C, Ma J and Li J 2022 *Comput. Ind. Eng.* **172** 108517
[34] Zhang Y H and Zhang T 2022 *Int. J. Bifurc. Chaos* **32** 2250127
[35] Zhu C and Ma J 2023 *Comput. Ind. Eng.* **181** 109309
[36] Tao F, Zhou Y, Bian J S and Lai K K 2023 *Ann. Oper. Res.* **324** 601
[37] Pal B, Sarkar A and Sarkar B 2023 *Expert Syst. Appl.* **211** 118315
[38] Wang C, Pi J X, Zhou D, Tang W and Yang G H 2023 *Physica A* **618** 128691
[39] Zhou W and Liu H Z 2023 *Commun. Nonlinear Sci. Numer. Simul.* **118** 107029
[40] Chen J, Hou R, Xiao L, Zhang T H and Zhou Y W 2023 *Chaos, Solitons and Fractals* **168** 113158
[41] Wei Z C, Tan W, Elsadany A A and Moroz I M 2023 *Nonlinear Dyn.* **111** 17561
[42] Fan, R G, Lin, J and Zhu K W 2019 *Physica A* **528** 121460